AD-A038 910 AIR FORCE INST OF TECH WRIGHT-PATTERSON AFB OHIO SCH--ETC F/G 18/2
ISOTOPIC ANALYSIS OF LOW-ACTIVITY PLUTONIUM SAMPLES USING HIGH---ETC(U)
DEC 76 J L STRICKLAND
UNCLASSIFIED AFIT/GNE/PH/76D-7 NL

1 OF 1
AD A038910

END

DATE FILMED
5-77

UNITED STATES AIR FORCE
AIR UNIVERSITY

AIR FORCE INSTITUTE OF TECHNOLOGY

Wright-Patterson Air Force Base, Ohio

(1)

ISOTOPIC ANALYSIS OF LOW-ACTIVITY PLUTONIUM SAMPLES USING HIGH-RESOLUTION ALPHA AND PHOTON SPECTROSCOPY

THESIS

GNE/PH/76D-7

Jack L. Strickland
Captain USAF

Approved for public release; distribution unlimited.

ISOTOPIC ANALYSIS OF LOW-ACTIVITY PLUTONIUM SAMPLES USING HIGH-RESOLUTION ALPHA AND PHOTON SPECTROSCOPY

THESIS

Presented to the Faculty of the School of Engineering

Air Force Institute of Technology

Air University

in Partial Fulfillment of the

Requirements for the Degree of

Master of Science

By

Jack L. Strickland
Captain USAF

Graduate Nuclear Engineering

December 1976

Approved for public release; distribution unlimited.

Preface

This thesis is concerned with the measurement of $^{239}Pu/^{240}Pu$ ratios in an isotopically mixed sample by using high resolution alpha and photon spectroscopy. It demonstrates an attempt to use alpha-gamma coincidence spectroscopy and singles, alpha particle and L x-ray spectroscopy to determine these ratios for low activity samples of less than 2000 DPM. Coincidence spectroscopy proved to be unfeasible at these activity levels, and statistically significant results were not obtained from the singles method; however, procedures were developed in this experiment that should allow a continuation of the experiment to provide improved results.

I wish to thank several people for their contribution to this thesis. My sincere gratitude goes to Dr. Richard Hagee, my thesis advisor, and Dr. George John with whom I discussed my progress, my difficulties and eventually my results, and to Lt. Col. Savery Stuckey and Capt. Ronald Jefferies of McClellan Central Laboratory for their interest in this project and support in supplying isotopic samples on a moments notice. I would also like to thank Capt. Piltingsrud and Capt. Stencel of the USAF Radiological Health Laboratory in verifying a gamma spectrum acquired of one low-activity sample by a run in their low-background chamber, and Mr. Roland Armani of Argonne National Laboratory in supplying two high-activity ^{240}Pu samples for calibration sources. Finally, but certainly not least, a very special word of thanks is devoted to my wife Judy, who typed this thesis and whose affection and understanding saw me through this project.

Contents

Contents (cont.)

List of Figures

List of Figures (cont.)

List of Tables

Abstract

High-resolution alpha particle and photon spectroscopy is applied to determining the ratios of ^{239}Pu and ^{240}Pu in isotopically mixed samples of less than a few thousand disintegrations per minute. The utility of alpha-gamma coincidence spectroscopy in measuring ratios of ^{239}Pu to ^{240}Pu is explored. Experimental equipment, procedures and calibration methods are discussed. Minimum activity levels necessary for detection and quantification are presented for the equipment used in the experiment. The minimum activity level for quantification for an eight-hour acquisition time was found to be at least 20,000 disintegrations per minute. A method of determining the $^{239}Pu/\ ^{240}Pu$ ratio is also presented for the use of singles alpha particle and L x-ray spectroscopy. This method is based upon differences in uranium characteristic x-ray intensities of the daughter nuclides of these two isotopes following the internal conversion process. A procedure is introduced for correcting a complex L x-ray spectrum for the presence of ^{241}Am in the sample and its contribution of neptunium characteristic L x rays to that spectrum. Instrumental and statistical uncertainties prevented reliable determination of isotopic ratios. Improvements in experimental equipment are recommended to reduce uncertainties. Major radiation intensities are tabulated for plutonium isotopes and for several other heavy elements.

ISOTOPIC ANALYSIS OF LOW-ACTIVITY PLUTONIUM SAMPLES USING HIGH-RESOLUTION ALPHA AND PHOTON SPECTROSCOPY

I. Introduction

In the fields of radiochemistry and health physics it is frequently desired to know the isotopic composition of samples containing actinide series elements. Since most radioactive actinides decay by alpha emission, alpha pulse-height analysis is routinely used to quantify the amount of a given nuclide in the presence of others. However, there are some nuclides that emit alpha particles with energies too close to one another to be resolved by alpha spectroscopy alone. ^{239}Pu and ^{240}Pu are two such nuclides that are often found together in varying ratios and for which there is no simple method for determining that ratio.

Background

The two isotopes of ^{239}Pu and ^{240}Pu emit alpha particles with energies that differ by only a few keV. Pulse-height analysis techniques using state of the art semiconductor detectors alone are inadequate in resolving these two isotopes, but instead yield only a sum count of the number of alpha particles emitted by both isotopes. The ratio can, however, be measured by mass spectrometry. The number of atoms of each isotope present may be determined from this ratio and the total alpha particles emitted, (determined by a spectrometer with known efficiency). While this procedure has proven reliable, it requires additional time and effort to prepare separate samples for both the alpha counting system and the mass spectrometer. If only one sample is present, recovery of the sample after mass spectrometric analysis is difficult. The overall

efficiency of the procedure for detecting and quantifying Pu ratios could be improved if the procedure could be reduced to a single measurement on a single sample.

Problem Statement

The purpose of this thesis was to explore and determine the feasibility of using high-resolution alpha and photon spectroscopy together to resolve the isotopes of heavy elements in general, and those of ^{239}Pu and ^{240}Pu in particular. The object was to find a method of determining these isotopic ratios by a relatively simple method without the use of a mass spectrometer.

Scope

The study was primarily experimental in nature and was restricted to applications of currently-available alpha and photon detection systems. The study also primarily addressed samples having low levels of activity. The activity levels varied from a few-tens to several thousand disintegrations per minute and were the guide for determining practical sensitivity levels for detection.

General Approach

Two approaches were studied; first, the techniques of coincidence spectroscopy were examined for applicability to the problem. Second, the information contained in alpha and photon spectra were examined to see if the information contained in each, when taken together, might provide sufficient information to calculate the isotopic composition of the sample.

Coincidence spectroscopy uses the output pulses of a coincidence circuit to turn on, or "gate", a multichannel analyzer for storage of a

pulse only when that pulse is in coincidence with a second pulse meeting certain criteria. Specifically, an alpha spectrum was acquired only when gamma radiation emitted by one of the isotopes present was simultaneously detected by a second detector.

The second approach was based upon the fact that although both Pu isotopes emit alpha particles and characteristic x rays(following internal conversion)of the same energy, the difference in their x-ray emission rates per alpha disintegration is sufficiently different that the disintegration rate of each isotope could be calculated.

Although the first approach proved to be negative at the activity levels of interest, the second approach appears to offer some promise. Using the procedures developed in this work, and perhaps a different detection system, one should be able to determine the $^{239}Pu/^{240}Pu$ ratio in a single measurement.

The remainder of this report is devoted to a detailed description of equipment and procedures used in this analysis. Chapter II provides the theory for the two approaches pursued. Chapter III gives a complete description of the experimental equipment and electronics. Chapter IV contains experimental procedures and calibration methods. Chapter V discusses the methods of data reduction and error analysis, and Chapter VI presents results, conclusions, and recommendations for future work.

II. Theory

Radioactive Decay Process

As is the case with many radioactive actinides, ^{239}Pu and ^{240}Pu decay by alpha emission to either ground or excited states of the daughter nuclei ^{235}U and ^{236}U respectively.

The simplified decay schemes depicting major branching of these two nuclides are shown in Figure 1. It must be noted that the decay schemes of these two nuclides are much more complex than shown with many higher excited levels of the uranium being infrequently populated by emission of lower energy alpha particles. (Ref 1:427,429).

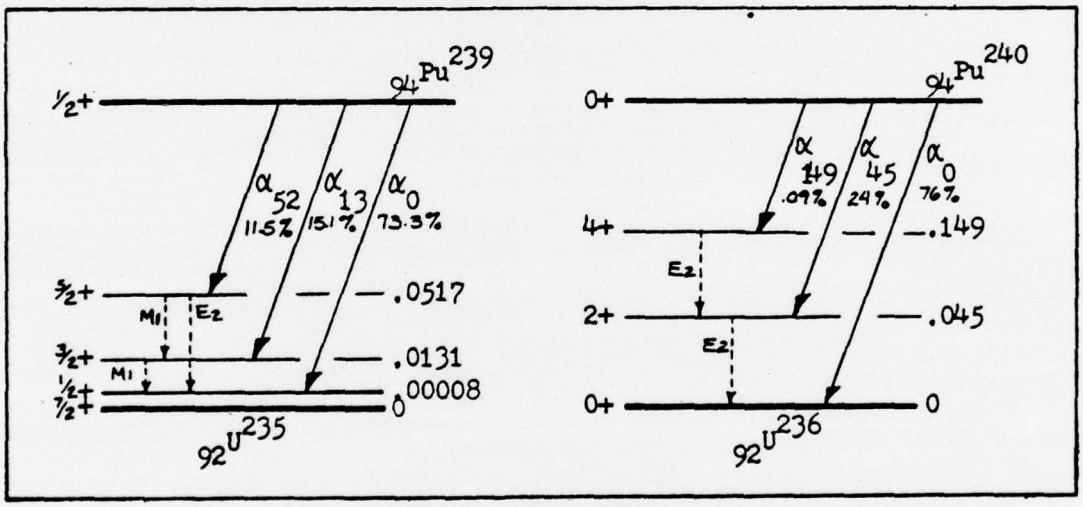

Figure 1. Decay Schemes for Plutonium Isotopes

Whenever a nucleus is formed in an excited state for which the excitation energy is insufficient for nuclear particle emission, the mode of deexcitation is by electromagnetic transition or internal conversion. The electromagnetic transition consists of the emission of a gamma ray. The internal conversion process is that of ejecting an orbital electron. The two processes are competitive and the ratio of internal conversion to

gamma emission is known as the internal conversion coefficient. This coefficient can be determined by rigorus quantum mechanical calculations, or determined by experimental measurement of internal conversion electron-to-gamma emission ratios. The conversion coefficient is dependent upon several factors. As the energy of the excited state increases, the internal conversion coefficient rapidly decreases. The conversion coefficient is strongly dependent upon the parity and spin differences of the excited and the ground state. Furthermore, the coefficient increases rapidly with atomic number, approximately as Z^3 over much of the range. In general, internal conversion is found most often in heavy elements when low energy gamma rays are emitted. (Ref 2:428).

A vacancy produced in an atomic shell from internal conversion causes electron transitions from outer shells, a cascade effect, where the law of energy conservation may be either satisfied by the simultaneous emission of a photon (characteristic x ray) or by the ejection of an electron from an outer shell (Auger electron). The x-ray emission and Auger transitions are also competitive, but x-ray emission is favored for elements of high atomic number.

The process of internal conversion follows the decay of the parent nuclide to the excited state of the daughter nuclide, thus in the case of plutonium alpha decay, x-ray emission is characteristic of the uranium nucleus. Although the process does follow alpha decay, the emissions of alpha particle and x rays are essentially simultaneous.

The lower excited energy states of uranium are highly internally converted; giving rise to many more conversion electrons and characteristic x rays than emitted gamma rays. A summary of major radiation abundances for some plutonium isotopes, along with those of several other heavy

elements, are tabulated in Appendix A. The most abundant gamma ray of ^{239}Pu is that of the 51.6 keV transition which is present in an abundance of 2×10^{-4} gamma rays per disintegration. In the case of ^{240}Pu, the most prominent gamma ray, 45 keV, is only slightly more abundant with 4.5×10^{-4} gamma rays per disintegration. In both of these plutonium isotopes, the most abundant photons are the L-series characteristic x rays from internal conversion which are approximately 100 times more abundant than the aforementioned gamma-rays (0.05 and 0.1 x rays per alpha disintegration respectively for ^{239}Pu and ^{240}Pu) (see Table I).

Table I

Major Radiation Energies and Yields in the Decay of ^{239}Pu and ^{240}Pu

^{239}Pu			^{240}Pu		
Radiation	Energy	Absolute Yield	Radiation	Energy	Absolute Yield
α_0	5.151 MeV	0.733	α_0	5.168 MeV	0.76
α_{13}	5.145	0.151	α_{45}	5.123	0.24
α_{52}	5.107	0.115	α_{149}	5.020	0.0009
γ_2	38.6 keV	5.9×10^{-5}	γ_1	45.23 keV	4.5×10^{-4}
γ_4	51.6	2.1×10^{-4}	γ_2	103.6	7.0×10^{-5}
γ_{14}	129.27	6.2×10^{-5}	γ_3	160.35	4.2×10^{-6}
L_ℓ(U)	11.618 keV	0.0011	L_ℓ(U)	11.618 keV	0.0024
L_α(U)	13.615	0.0182	L_α(U)	13.615	0.0378
L_β(U)	17.220	0.0216	L_β(U)	17.220	0.0484
L_γ(U)	20.167	0.0053	L_γ(U)	20.167	0.0120
ΣL(U)	11.6-20.1	0.0463	ΣL(U)	11.6-20.1	0.1006

Coincidence Spectroscopy

As was mentioned in the previous section on radioactive decay processes the primary radiation of a nuclide is often accompanied by secondary radiation of the daughter nuclide. The simultaneous detection of two or more of these primary and secondary radiations by different detectors can consequently yield valuable information about the decay transitions and about the excited energy states of the daughter nuclide. Coincidence spectroscopy is one such method that utilizes the simultaneity of detection to determine decay schemes, or decay rates of samples. When used to determine the decay rate, the method is more applicable when applied to a radiochemically pure sample.

If a transition α is registered in one detector with an efficiency ϵ_α, and in a second detector a transition γ is registered with efficiency ϵ_γ, and further assuming that both are insensitive to the radiation detected by the other, then the number of counts in each detector in a given time T for a sample with a constant decay rate R decays per unit time is

$$N_\alpha = \epsilon_\alpha \alpha RT \quad ; \quad N_\gamma = \epsilon_\gamma \gamma RT \tag{1}$$

If one further assumes isotropic angular correlations between the two radiations and a coincidence efficiency of 1., the registered number of coincidences recorded in the two detectors is

$$N_{\alpha\gamma} = \epsilon_\alpha \epsilon_\gamma (\alpha\gamma) RT \tag{2}$$

where α and γ are taken as transition intensities. This number of coincidences includes coincidences that occur by change due solely to

the finite resolving time of the coincidence circuit, τ. It can be shown (Ref 3:543) that the number of random, or chance coincidences is

$$N_R = 2\tau (N_\alpha - N_{\alpha\gamma})(N_\gamma - N_{\alpha\gamma})/T \tag{3}$$

or when $N_{\alpha\gamma}$ is small compared to N_α and N_γ, as is often the case, then

$$N_R = 2\tau N_\alpha N_\gamma / T \tag{4}$$

The true coincidences are essentially the observed coincidences corrected for chance coincidence, dead time losses, and background.

The power of the coincidence technique is that the decay rate of the sample can often be calculated without direct knowledge of the individual detector efficiencies. Combining equations (1) and (2), the decay rate, R, of a sample is given by

$$R = N_\alpha N_\gamma / N_{\alpha\gamma} T \tag{5}$$

The above formula however, necessitates that the radiations α and γ are both from the same nuclide. In the case of isotopically-mixed samples, this assumption is seldom true and both transitions α and γ are the combined transitions of two or more isotopes.

An inherent disadvantage in coincidence spectroscopy is that it incorporates the efficiency of both detectors to register a count. The total efficiency for a coincidence being the product of individual detector efficiencies; consequently, the number of coincident counts could be small and the acquisition times large for a low-activity sample or for a low-geometry detection system. An advantage is that it reduces background substantially.

In the particular case of mixed samples containing both ^{239}Pu and ^{240}Pu, selective acquisition of the alpha spectrum from ^{239}Pu was attempted by gating on the 51.6 keV gamma ray emitted by this isotope. The activity of ^{239}Pu could then be calculated with knowledge of the efficiency of the gamma-ray detector and the abundance of gamma rays per disintegration. However, a problem arises in identification of the gamma ray that is to serve as the pulse to trigger the gate. With abundances as low as they are for the 51.6 keV gamma ray of ^{239}Pu it could well be undetected or hidden in the background.

Singles Spectroscopy

Just as the alpha spectrum of ^{239}Pu is unresolvable from that of ^{240}Pu, so also is the uranium characteristic x-ray spectrum arising from the decay of both isotopes. However, the fact that the ratio of total L x rays per alpha transition for ^{240}Pu is approximately twice that ratio for ^{239}Pu theoretically provides one with sufficient information from the two singles spectra of alpha particles and L x rays to calculate the ratio of ^{239}Pu to ^{240}Pu in a given sample.

If one takes α_T as the total alpha counts under the 5.15 MeV to 5.17 MeV alpha peak as being a sum of the individual α counts of ^{239}Pu and ^{240}Pu and similarly defines X_T as the total L-shell characteristic x rays from internal conversion of the two isotopes then

$$\alpha_T = \alpha_{239} + \alpha_{240} \tag{6}$$

$$X_T = X_{239} + X_{240} \tag{7}$$

From recent studies at Oak Ridge National Laboratories, (Ref 4:578), and Argonne National Laboratories, (Ref 5), the ratios of L x rays to alpha disintegration have been well documented for ^{239}Pu and ^{240}Pu:

$$\frac{X_{239}}{\alpha_{239}} = 0.046 \qquad \frac{X_{240}}{\alpha_{240}} = 0.101 \tag{8}$$

By substituting these last two ratios (8) into equation (7) and then solving simultaneously with equation (6), one obtains the activity ratio of ^{239}Pu to ^{240}Pu in terms of the counts under the alpha peak and under the L x-ray spectrum.

$$\frac{\alpha_{239}}{\alpha_{240}} = \frac{0.101\,\alpha_T - X_T}{X_T - 0.046\,\alpha_T} \tag{9}$$

The atom ratio of these two isotopes can be calculated from the activity ratio by use of the decay coefficients:

$$\frac{^{239}Pu}{^{240}Pu} = \frac{\lambda_{240}\,\alpha_{239}}{\lambda_{239}\,\alpha_{240}} \tag{10}$$

III. Experimental Equipment and Electronics

Introduction

The initial thrust of this project was directed to the use of alpha-gamma coincidence spectroscopy. Consequently, the selection of equipment and the design of apparatus were influenced by the need to maximize efficiencies and geometries for detection of these particular radiations. Because of the low activity of the samples, a concentrated effort was made from the beginning to reduce background radiation.

When later experimental efforts turned toward singles spectroscopy of both alpha particles and L-series x rays, the equipment used for alpha spectroscopy in the original coincidence experiment was retained and a detector and spectroscopy circuit were incorporated for the x rays.

Equipment

The low penetration capabilities of alpha particles in air generally requires that alpha spectroscopy be accomplished with the sample and detector in an evacuated chamber. The coincident detection of gamma rays from the same sample requires that a second detector be capable of "seeing" the sample simultaneously.

The major design problem concerned the configuration of the chamber and sample mount to allow both alpha and gamma detectors to "see" the sample and to maximize the solid angles for each detector.

Vacuum Chamber. Samples of heavy elements from McClellan Central Laboratory (MCL) consist of the isotopic material electrodeposited on 3 mil-thick platinum disk of approximately 2.2 cm diameter. The diameter of the area of deposition is 1.7 cm. A sample mount that would hold the disk by the outer edge close to the alpha detector, and yet

would not further attenuate the gamma radiation exiting the backside of the sample, appeared to offer the best geometry for both detectors. Because of the $1/R^2$ dependence of solid angle on sample-to-detector distances, these distances were reduced to absolute minima allowing only for slight variations in sample configuration and detector size. The completed assembly consisted of an aluminum cylinder, one inch high by four inches in diameter. The alpha detector was attached on-axis, internally at one end of the chamber. The endplate of the chamber served as sample mount, vacuum seal, and exit window for gamma radiation and had a beryllium window of 7/8 in. diameter and a thickness of 20 mil. A detailed drawing of the chamber is presented in Appendix B.

With the endplate in place, the active side of the sample disk was 5.5 mm from the face of the alpha detector. With the gamma detector directly against the chamber, the distance from sample to detector entrance window was 4.0 mm. (The sensitive surface of the detector was another 8.0 mm behind the window).

The combined chamber and detector assembly was inserted within a cylindrical lead shield of $1\frac{1}{4}$ in. thick sides. (see Fig. 2). One end of the cylindrical lead chamber was shielded with a removable lead plate of one in. thickness.

A graded shielding consisting of a 25-mil-thick copper sleeve was inserted between lead shield and aluminum chamber to absorb x rays induced in the outer lead cylinder.

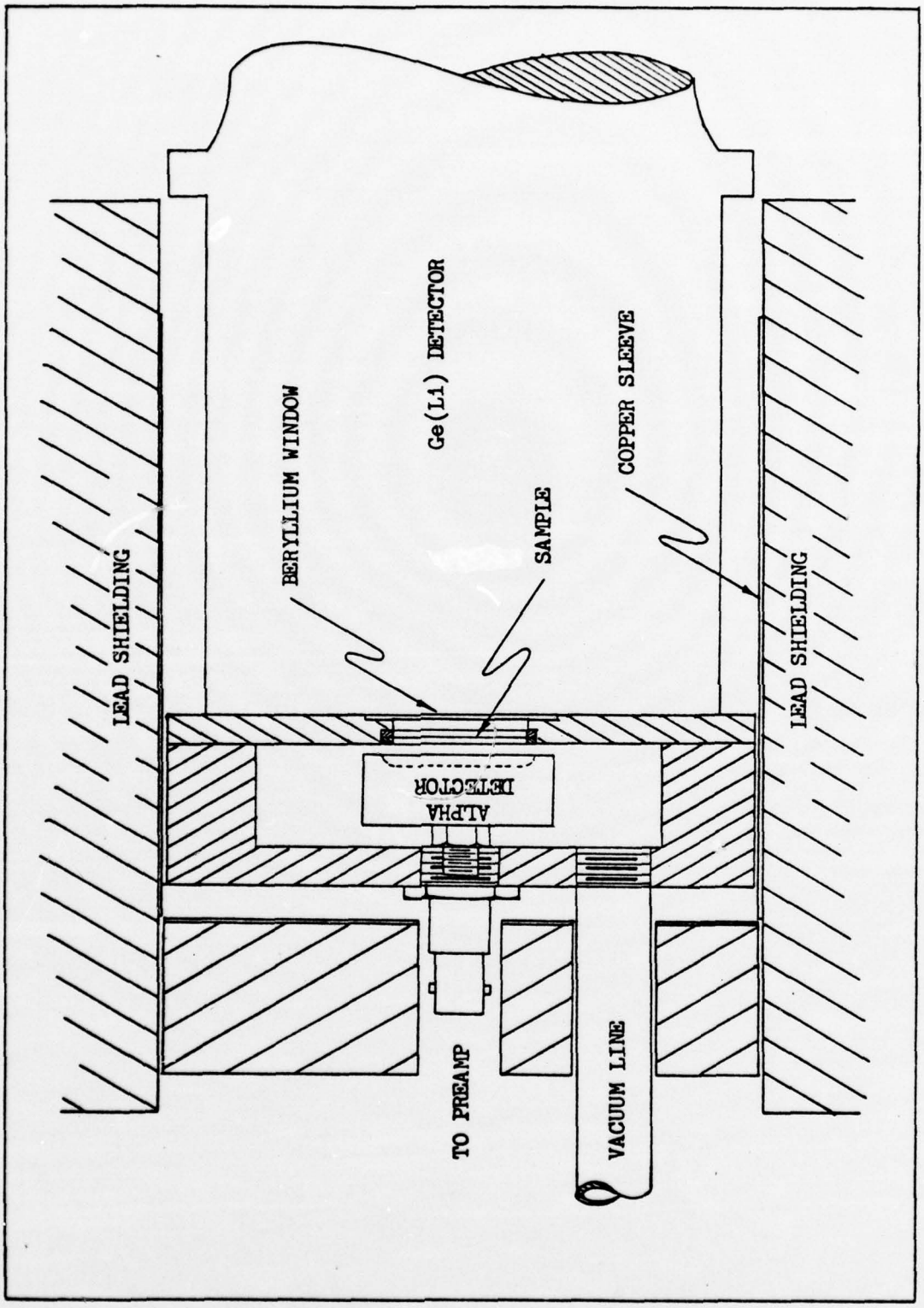

Figure 2. Vacuum Chamber and Detector Arrangement

Detectors. The detector originally used for alpha spectroscopy was an ORTEC, Model A-020-100-100 partially-depleted, silicon surface-barrier detector with an active area of 100 mm^2 and a depletion depth of 100μ . It was chosen for its compact size, short charge-collection times, and excellent energy resolution (total measured system resolution was 25 keV FWHM at 5.49 MeV). It further provided for a geometry factor, $\Omega/4\pi$, of 0.125 (where Ω is the solid angle in steradians).

Later, the detector was replaced by a larger ruggedized silicon surface-barrier to increase the geometry factor. An ORTEC Model BR-25-450-100 with an active area of 450 mm^2 and a depletion depth of 100μ was chosen. Due partially to its thicker aluminum entrance window and larger surface area, the system resolution was reduced to 45 keV FWHM at 5.49 MeV. The decrease in resolution did not hamper resolving the alpha particles of interest and the two-fold increase in efficiency (geometry factor of 0.258) was highly desirable in reducing the acquisition times for spectra of lower-activity samples.

The detector selected for gamma-ray spectroscopy was a lithium-drifted, germanium, Ge(Li), detector of right-angle-cryostat-configuration. The detector was chosen because of its excellent energy and timing resolutions (system energy resolution was measured at 2.8 keV FWHM at 122 keV) and further because of its thin beryllium entrance window, providing for high transmittance of low-energy photons. The sensitive surface of the detector diode had an area of 5.0 cm^2 and was mounted 8.0 mm behind the entrance window. With the detector window physically against the beryllium window of the vacuum chamber, the geometry factor for photon detection was 0.139.

Electronics

The block diagram for the coincidence circuit is shown in Fig. 5 Appendix B.

Amplifiers. The preamplifier for the Nuclear Diode Ge(Li) detector was integral to the detector housing and provided connections for detector bias voltages as well as for signal inputs to the linear amplifier. The preamplifier used with the surface barrier detector was an ORTEC Model 109A with a low-noise FET input stage.

The linear amplifiers amplify and shape the output pulses of the preamplifiers to obtain optimum timing and energy resolution. Tennelec Model TC 203 BLR linear amplifiers were chosen for both the alpha and gamma channels. This insured similar output pulse shapes and signal processing times.

Coincidence Circuitry. Bipolar outputs of the linear amplifiers were fed into timing single channel analyzers (TSCA) for differential or integral energy discrimination and also as a means of inserting timing delays in either channel prior to the coincidence unit. The outputs of the TSCA's were fed into an ORTEC Model 414A, fast coincidence unit, which generates a logic pulse output if the cross over-times of the two input pulses are within the resolving time of the circuit(continuously variable from 10 nsec to 110 nsec). The output of the fast coincidence unit was fed into an ORTEC Model 416A gate-and-delay generator which translates the logic pulse of the coincidence unit into output pulses of selectable amplitude and width. The output pulse of the gate and delay generator was fed directly to the gate input of the multichannel analyzer (MCA).

Spectroscopy Circuit

The monopolar output pulse of the linear amplifier for the alpha channel passed through a delay amplifier which delayed the output sufficiently to compensate for the time required for the coincidence circuits to process inputs. The output of the delay amplifier was connected to an ORTEC Model 408 biased amplifier which expanded regions of interest in the spectrum and its output was routed directly into the signal input of the MCA. Three counter timers were used to provide continuous singles counting. These were monitored to determine approximate sample activities, to aid in trouble shooting, and to provide the singles rates for the random coincidence corrections of equation (4). Two scalers, RIDL Model 49-43, were used to record singles counts for the alpha and gamma channels. The other counter, a Canberra Model 1771, recorded total coincidences.

X-Ray Spectroscopy

The spectroscopy circuit assembled for x rays is similar to the circuitry for alpha spectroscopy, previously mentioned. (see Fig. 6, Appendix B). The detector chosen was the Princeton Gamma-Tech Model LS-33 lithium-drifted silicon, Si(Li), detector. It was chosen because of excellent resolution and high efficiency for low-energy (<30 keV) photon detection. The choice was made between the Si(Li) and an available intrinsic germanium detector primarily on the shorter distance from entrance window to sensitive detector area for the Si(Li) detector. This shorter distance provided for a higher total efficiency. Another factor in choosing the Si(Li) over the germanium was an observed lower background for the Si(Li). Both detectors had active areas of 30 mm^2 and resolutions for the two were comparable: 200 eV FWHM @ 6.4 keV for Ge and 230 eV FWHM

@ 6.4 keV for the Si(Li) detector. The germanium, because of its higher atomic number, provided for higher detection efficiencies for photons greater than 30 keV, where the efficiency of Si(Li) drops off rapidly, but since the L x rays of uranium range in energy from 11-21 keV, this was of no concern.

The preamplifier of the x-ray detector was built into the cryostat assembly and its output was fed to a Princeton Gamma-Tech Model 340 linear amplifier. The output of the linear amplifier was fed into a Tennelec Model TC601 strobed pulse stretcher, which provided for better energy resolution in shaping the pulse to that compatible with the MCA. A biased amplifier was inserted between pulse stretcher and MCA to expand the 11 keV to 21 keV spectrum of interest to a full scale range on the MCA.

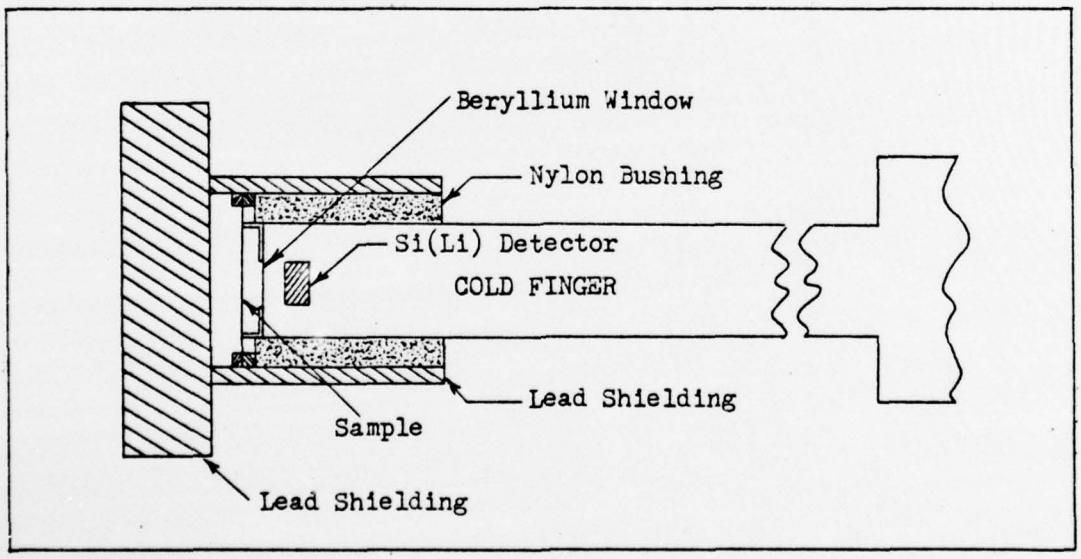

Figure 3. Sample Mount for X-Ray Detector

The x-ray detection system required a sample mount that would hold the source against the detector housing in a reproducible geometry. The final design consisted simply of a nylon sleeve that fit snugly over the detector housing. The sample was held onto the end of the sleeve by a 1/16 in. thick piece of lead wrapped around the outside of the sleeve. The front of the detector was shielded by an additional piece of 1/8 in. thick lead. The entire assembly was of light weight, provided sufficient shielding for low-energy photons and yet permitted an easy change of samples. (see Fig. 3)

IV. Experimental Procedures : Calibration and Data Collection

Several calibration measurements were necessary before raw spectral data could be identified or quantified. Most calibrations were a one-time accomplishment, still others had to be checked periodically for changes in system response. Whenever any change in a component was deemed necessary, a careful analysis of the impact on the system was essential to assess the necessity of a recalibration.

Energy Calibration

Calibrations are necessary to relate energy to channel number for the pulse height spectra collected by the MCA. This is generally a one-time measurement for each detector-amplifier combination; however, it must be repeated with any change in detector, amplifier component, detector bias, or amplifier gain. The energy calibration techniques of the system for alpha, gamma, and x-ray radiation are all quite similar, in that, all use sources emitting radiation of referenced energies. The choice of particular sources used were dependent upon the full-scale energy range of interest.

Alpha Spectroscopy. Several alpha reference sources were available for energy calibration: ^{241}Am, ^{238}U, ^{233}U; however, the most useful source for much of this work was an isotopically mixed sample from MCL containing ^{242}Pu, ^{243}Am, and ^{244}Cm and providing alpha energy peaks of about 4.9, 5.3, and 5.8 MeV respectively. This sample contained several thousand DPM of each nuclide electrodeposited on the standard Pt disk and allowed rapid, high-resolution determination of peak channels. These reference peaks spanned the energy range of interest very well.

It was possible, after initial energy calibration, to maintain a continuous cross check of energy calibration by reference to the peaks of ^{239}Pu, ^{240}Pu and ^{241}Am normally present in each sample being analyzed.

Gamma Spectroscopy. For gamma-ray energy calibration the range of energies being analyzed was generally confined to that less than 150 keV. The most convenient sources were found to be those of ^{57}Co, ^{109}Cd, and ^{241}Am. These three isotopes provide photon reference peaks of 14.4, 22, 59.5, 87.7, 122 and 136 keV.

X-Ray Spectroscopy. For initial energy calibration, the sources of ^{57}Co and ^{109}Cd providing photon energies of 6.4, 7.05, 14.4, and 22 keV from gamma transitions and characteristic x rays were most useful. After expansion of the spectrum to the energy range of interest; (11-21 keV) by the biased amplifier, the L_α, L_β, and L_γ x rays from internal conversion in Np following the decay of ^{241}Am were used for follow-on monitoring of energy calibration.

To these several reference points of energy-vs.-channel-number for each of the above three spectra, a least-squares, straight line was fit using the linear regression routine of a Texas Instrument SR-51 hand calculator. The slope of the line and intercept were used to determine the energy of peaks so they could later be identified.

Efficiency Calibration

The method for efficiency calibration of alpha, gamma and x-ray detectors is essentially the same, in that all were calibrated by reference to samples of a known activity. Each detector calibration, however, offered its own particular problem and difficulty.

Alpha Particle System. The large ruggedized surface-barrier detector was calibrated for efficiency by reference to the supplied activity figures of three separate samples supplied by MCL. These were mounted in the standard geometry configuration in the chamber. Table 1 lists the sample by number and the activity for each isotope present. The uncertainties in the calculated efficiencies are the standard deviations and include the uncertainty in sample activity as well as the statistical uncertainty in the measured count rate.

Table II

Calculated Total Efficiencies for Standard Alpha Sources

Sample #	Nuclide	Alpha Energy (MeV)	Corrected Activity (DPM)	Total Efficiency
Cm-1	^{242}Pu	4.90	3214±15	0.255±.002
	^{243}Am	5.27	3182±15	0.257±.003
	^{244}Cm	5.81	1894±11	0.249±.003
Pu-02	^{242}Pu	4.90	632±6	0.270±.003
	^{239}Pu	5.15	689±7	0.263±.003
	^{238}Pu	5.49	54±2	0.283±.010
Pu-03	^{239}Pu	5.15	460±6	0.254±.002
	^{236}Pu	5.77	405±5	0.277±.003

The above efficiencies appeared to have no energy dependence and were consequently averaged to give a value of: 0.264±.004. The intrinsic efficiency for alpha particles incident on the face of the detector was initially assumed to be very close to 100%.

A program SOLIDA was written that would calculate the solid angle for a circular disk source on axis and at a given distance from a circular disk detector, (see Appendix C). This geometry factor was then compared to the measured efficiency. Using the area of sensitive region of the detector, the area of deposition, and the source-to-detector distance; the geometry factor was calculated to be 0.258±.008. This figure was only slightly lower than the measured total efficiency of 0.264±.004. The difference was within expected statistical variations; however, the factor of 1.02 difference in the two was examined for a backscattered contribution from the platinum backing. A. H. Snell gives values as high as 1.04 for backscattered alphas from a Pt backing when detected in a 2π geometry (Ref 13:336). Siegbahn, however, states the contribution from backscatter in a point source-detector geometry of π steradians is negligible, since most backscattered alpha particles depart the surface at low angles (Ref 3:428). Since the sample-detector geometry for this experiment cannot be represented by a point source, some backscattered alpha particles may be incident on the detector.

Gamma-Ray System. The problem of efficiency calibration for photon detection is not as easily handled as that for alpha particle detection. The problem arises from the highly dependent nature of photoelectric absorption on photon energy. As the energy of the photon increases, the photoelectric coefficient decreases. On the other hand, as the photon energy decreases, the more it is attenuated by the detector window, air between sample and detector, and by self absorption of the sample material itself. Consequently, photon total efficiency curves are characterized by curves that drop off at both ends of the energy spectrum.

For the particular case of the gamma rays in this experiment, the area of interest was a narrow range of energies on either side of the 51.6 keV gamma ray of ^{239}Pu. This range was primarily limited to 40 to 150 keV and gamma-ray standards supplied by NBS were sufficient to define the calibration curve over this range. The photopeak efficiency curve derived from ^{57}Co, ^{109}Cd, ^{241}Am, and ^{137}Cs after corrections were made for source-geometry differences and window absorption is plotted in Fig. 7.

X-Ray System. Accurate efficiency calibration for the x-ray detector was most difficult. Much of the uncertainty in the final results of this experiment is due to the uncertainty of this efficiency. The problem primarily arises as a result of the scarcity of standardized samples which emit gamma rays or x rays in the lower energy ranges (<40 keV). The gamma-ray standards, ^{57}Co, ^{137}Cs, and ^{109}Cd, are primarily used to calibrate gamma-ray detectors over a higher energy of 50-660 keV; however, these sources also emit x rays, the intensities of which have to be derived from internal conversion coefficients and fluorescent yields. Larger uncertainties have to be attached to these emission rates than that of the primary gamma rays. Moreover, since the sources are primarily higher energy gamma standards, the sandwiching material of the sample can greatly effect the emission rates of the lower energy photons. (Ref 6:207-208). The small entrance window of the Si(Li) detector made sample alignment very critical. The areas of deposition for these gamma-ray standards were nominally 2-3mm in diameter but small shifts off axis could greatly effect the geometry and resulting efficiency data.

The most accurate approach appeared to be that of measuring characteristic x rays of Np from internal conversion following the decay of

^{241}Am (Ref 6:215). Two americium-241 standards issued by NBS and NEN (New England Nuclear Co.) were employed for this measurement. These sources were better than the aforementioned gamma-ray sources because as alpha sources they were not sandwiched in polyethylene. The standardized activities of the samples were decay corrected and the absolute intensities of x rays per disintegration used were those of Campbell and McNelles (Ref 6:215).

After correcting for geometry differences and window absorption, the resulting efficiencies were plotted vs. energy with those determined by the gamma-ray standards (see Fig. 8). The discrepancy in the two efficiency curves derived from the two types of standards were never resolved despite repeated measurements.

The efficiency data derived from the Np x rays were used to quantify x ray abundances of ^{239}Pu and ^{240}Pu in this experiment. It was felt that the very small energy difference in characteristic x rays of Np and U would introduce less error for efficiency than that of the interpolated curve derived from the wider spread energies of the gamma ray standards.

Relative Delay Calibration

The relative delay of the gamma-ray and alpha particle detector signals being fed to the coincidence unit is of prime importance in determining the total coincidence count rate. These two signals must arrive at the coincidence unit within a very short time interval to insure operation at the maximum coincidence rate. Failure to operate at or near this maximum rate significantly decreases the total number of coincidences and increases the relative contribution of random coincidences to the total coincidence count.

This optimum relative delay was determined by varying the delay of the signal in one branch of the coincident circuit by the delay potentiometer of the TSCA. A source that emitted a relatively high number of alpha particles in coincidence with gamma rays was placed in the vacuum chamber for simultaneous alpha particle and gamma-ray detection. A curve of coincident counts vs. relative delay was then plotted for a 110 nsec resolving time setting on the fast coincidence unit. (see Fig. 9). The measure of FWHM of the delay curve provides the resolving time, 2τ, of the coincidence circuit. It is advantageous to make the resolving time as small as possible to reduce the number of chance coincidences. It should not, however, be reduced to a value that would lower the coincidence efficiency less than 100%. When the delay curve has a flat top, one can usually feel confident that the coincidence efficiency will be nearly equal to one. (Ref 3:554).

Data Collection

For coincidence spectroscopy when gating off a particular energy gamma ray, the upper and lower level discriminators of the TSCA must first be set to establish the energy window. If the window is set too narrow, true coincidences will be lost. If the window is too wide or displaced from the gamma-ray energy of interest, an excessive number of unwanted coincidences will be counted. This window is set by placing the TSCA in differential mode and routing its output directly to the gate input of the MCA. This permits gating on the same spectrum being acquired by the MCA. By varying the lower level discriminator and ΔE during acquisition of a gamma-ray spectrum, the spectrum can be limited to that of the desired energy window.

After setting the energy window, the acquisition of the gated spectrum is simple and only entails setting of the desired acquisition time.

V. Data Reduction and Error Analysis

Coincidence Spectroscopy

The very low intensity of gamma rays emitted in the decay of ^{239}Pu and ^{240}Pu, plus the low activity levels of the samples themselves, contributed to the unfeasibility of alpha-gamma coincidence spectroscopy at these activity levels. The number of coincident counts recorded in any one channel over a 48-hour period was never more than three; consequently, there were not any significant data to be reduced. Data reduction for these spectra consisted of calculating the contribution of random coincidences to the total coincidence spectrum. This was done by using equation (4), Chapter II, to calculate the predicted number of coincident counts in the acquisition period. Had this number ever been significant, a random coincidence spectrum would have been obtained. This would have been accomplished by setting the relative delay in one branch of the circuitry approximately .5 μsec off of the delay curve plateau. The acquired spectrum would then have been due to chance coincidences only.

Singles Spectroscopy

Quantification of a given radiation emitted by a sample consisted of: totaling the number of counts under the energy peak; subtracting the background contribution; then dividing this net count by the total efficiency of the detector.

Alpha Spectra. Determining the number of alpha particles emitted by a sample in a given period of time was a simple process of subtracting a pre-measured background spectrum from the gross count spectrum and dividing by the source detector efficiency. The resolution of the

detector, and the quality and uniformity of the samples were sufficient that the energy peaks of ^{241}Am and ^{238}Pu were resolvable from the combined $^{239}Pu/^{240}Pu$ energy peak. It was, therefore, unnecessary to correct for tailing contribution to adjacent peaks as in the case of low-resolution systems (Ref 9:1352). The background had to be periodically measured throughout the experiment because of increases in chamber and detector contamination from the Pu samples.

X-Ray Spectra. Determination of the net number of counts under an energy peak of the x-ray spectrum was more involved than that for alpha spectroscopy. The background for photon spectroscopy, is in general, very source dependent. It includes, in addition to natural background, that due to scattered radiation of the source itself.

There was neither a simple not accurate method of predetermining the background spectrum prior to the actual acquisition of the sample spectrum. The background was, instead, determined in a paired observation with the sample spectrum. For the case of the lower activity samples ($\sim$ 1000 DPM), the acquired peak counts, as well as background, were low for even extensive counting periods of 48 hours (see Fig. 11). The background counts in these cases were averaged over a twenty-channel span at five or six places throughout the spectrum between peaks. It was determined that this background could be approximated very well by a straight line. A least-squares straight line was fit to these five or six background points and the line was subtracted from the gross spectrum producing the net number of counts under each peak. Poisson statistics were used in calculating the uncertainties in background and peak counts, and the error was propagated in subtraction. (Ref 12:56).

The above procedure was satisfactory for determining the number of counts under a U L x-ray peak for an elementally pure sample. Often, however, the spectrum consisted of unresolved complex peaks from the contribution of other actinide characteristic x rays. ^{241}Am is one such isotope often found in Pu samples. The alpha decay of ^{241}Am is followed by the emission of Np characteristic x rays. The L x ray intensity for ^{241}Am is nearly four times that of ^{240}Pu and more than eight times that of ^{239}Pu (Ref 4:580). If the difference in decay rates of these isotopes is considered, the contribution of Np x rays to the compound Np/U x-ray spectrum could be significant with only a small atom abundance of ^{241}Am in the sample. Alpha particle spectroscopy can be used to determine ^{241}Am content unless ^{238}Pu is present too. The alpha groups of these two isotopes are also unresolvable. In the past, gamma-ray spectroscopy has been used effectively in determining ^{241}Am content in a Pu sample (Ref 7:198) (Ref 8:1759); however it has necessitated the calibration of a detector for gamma rays. The detection efficiency for 59 keV photons by a Si(Li) detector is very low, so this would effectively require a Ge or Ge(Li) detector. A method for spectrally subtracting the NP L x-ray contribution from the compound spectrum would be valuable in accurately quantifying U L x rays when only a Si(Li) detector is in use.

In spite of the compound nature of the NP/U L x-ray spectrum, the L_{α_1} peaks of NP and U were sufficiently resolved that a spectrum of gaussian peaks could be fit to the individual Np L x-ray lines based upon the intensity of the Np L_{β_1} peak. This theoretical spectrum for Np L x rays following ^{241}Am decay was generated by program SPECTRA (see Appendix D) using energies and relative intensities of Np L x-ray sub-group lines provided by Hyde (Ref 11:253-254). This same program

performs a third-degree, least-squares polynomial fit to the background, adds the background and Np L x-ray spectrum then substracts that sum spectrum from the compound Np/U L x-ray spectrum. The remaining spectrum is that due only to U L x rays. The counts under these peaks were then totaled and quantified.

The above procedure of spectra "stripping" was necessitated by the lack of literature on individual U L x-ray line intensities following Pu alpha decay. The subgroup intensities of L_ℓ , L_α , L_β and L_γ have been documented (Ref. 5) (Ref 4:580) and the energies are well known but subgroup x-ray line intensities are needed to predict a theoretical U x-ray spectrum.

CURVFIT, an interactive graphics program that fits either linear or nonlinear functions to a set of data points was used in an attempt to determine its utility for quantifying U L x rays in a complex spectrum. Its major limitations were that it could handle only 200 channels of data points at one time and was limited to a function of ten or fewer independent variables. With energies and standard deviations specified, this would allow ten Gaussian peaks to be fit by amplitude variations or only five peaks if both amplitude and energy were varied in the fit. With the amplitudes supplied by the program, the areas under the peaks could then be calculated by a separate program. Because of the 1024 channels used for the x-ray spectra and the complexity of peaks that must be fit, the program was found to be only marginally useful.

Error Analysis

The uncertainties associated with quantification of radiation depend upon the statistical uncertainties of the counting process, as well as those of source-detector efficiency. The first of these uncertainties

has been briefly covered in the preceding section; the second was more difficult to determine.

The geometry factor as calculated by SOLIDA depends upon three measurements: source radius, detector radius, and source-to-detector distance. The radius of the detector was calculated from the sensitive area of detector supplied by factory specifications. The radius of sample deposition was supplied, in the case of MCL samples, and measured for others. The source-to-detector distances were measured with a ruler. The 95% confidence interval of certainty was assumed to be within $\pm$0.5mm. The uncertainties associated with detector and sample radii, when supplied, were assumed to be small in comparison with the uncertainty of source-to-detector distance.

Geometry factors were calculated by SOLIDA for both the measured distances and for $\pm$0.5mm of the measured distances. The resulting range of efficiencies were taken as $\pm 2\sigma$ of the actual efficiency. This uncertainty was then propagated throughout future calculations involving the geometry factor.

Minimum Levels for Detection and Quantification

The usefulness of a procedure for the analysis of radioactivity is dependent upon the level of activity to which it is sensitive. It was felt that the results of this experiment would be more pertinent if minimum activity levels for detection and quantification were supplied for each method.

Numerous approaches, some of which are inconsistent, that define these limits are described in the literature. Currie of the National Bureau of Standards (Ref 14:586) provides a thorough discussion and working formulae for calculating these limits. Briefly, he defines three

specific levels of interest (1) L_c, the "decision limit" at which one may decide whether or not the results of the analysis indicates detection, (2) L_d, the "detection limit" at which a given analytical procedure can be relied upon to lead to detection, and (3) L_q, the "determination limit" at which a given procedure will be sufficiently precise to yield a satisfactory quantitative estimate. The degree to which the detection limit can be relied upon is established by a user-supplied acceptable confidence interval. The precision of the quantitative results determined at L_q is similarly defined by the standard deviation the user is willing to accept in the results.

Table III

Minimum Levels for Detection and Quantification

	L_c (counts)	L_d (counts)	L_q (counts)
Paired Observation $(\sigma_b^2 = \mu_b)$	$2.33\sqrt{\mu_b}$	$2.71+4.65\sqrt{\mu_b}$	$50\left\{1+\left[1+\frac{\mu_b}{12.5}\right]^{\frac{1}{2}}\right\}$
"Well-known" Blank $(\sigma_b^2 = 0)$	$1.64\sqrt{\mu_b}$	$2.71+3.29\sqrt{\mu_b}$	$50\left\{1+\left[1+\frac{\mu_b}{25}\right]^{\frac{1}{2}}\right\}$

These limits are naturally dependent upon the background and its uncertainty. Currie defines the "blank" as the signal resulting from a sample which is identical, in principle, to the sample of interest, except that the substance sought is absent (or small compared to the standard deviation of the blank). The blank as defined here is the background and represented by μ_b (the true mean of the blank) and its standard deviation σ_b. If the blank is determined in a paired observation with the signal, σ_b is not small in comparison to the deviation of the gross (signal + background) signal, σ_{s+b}.

On the other hand, if the background has been determined in a separate measurement to a high degree of precision, then the blank may be considered "well-known" and σ_b is small in comparison to σ_{s+b}. For radioactivity, observations are assumed to be governed by the Poisson distribution. Table III provides the working expressions for L_c, L_d, and L_q for radioactive analysis. The confidence is 95% in making the decision, "detected or not detected" and the relative standard deviation in the quantitative results at the L_q level is 10%.

VI. Results, Conclusions and Recommendations

The goal of this work was to explore methods and examine feasibilities of using high-resolution alpha and photon spectroscopy to resolve the two isotopes, ^{239}Pu and ^{240}Pu. The thrust of the effort was initially toward that of coincidence spectroscopy, however, the emphasis was later shifted to single alpha particle and x-ray spectroscopy. This goal has been partially obtained. Alpha-gamma coincidence spectroscopy has been determined unfeasible at the activity levels proposed in the scope of this experiment. Minimum levels for detection and quantification have been theoretically established for the coincidence technique when using the equipment assembled for this experiment. The results of alpha and L-shell x-ray singles spectroscopy are promising. Due to a poor sample-detector geometry, the efficiency calculations for x-ray detection have large associated uncertainties. These uncertainties plus statistical uncertainties from the small number of counts have consistently produced L x-ray to alpha disintegration ratios with errors too high for quantitative analysis of $^{239}Pu/^{240}Pu$ ratios. Due to time limitations of the experiment, these uncertainties have not been reduced and possible sources of other systematic errors have not been discovered. A valuable and large contribution to this analysis has been the approach and methodolology established in this experiment.

Coincidence Spectroscopy Discussion

To provide the highest geometry for both alpha and gamma-ray detection, the gamma rays were detected through the backside of the sample. Even the 3 mil-thick Pt disks, on which MCL routinely electrodeposit their samples, attenuate 40-50 keV photons greatly.

The transmittance is only 0.485 and 0.339 for 52 and 45 keV photons respectively. An improvement in transmittance however, was provided by a switch in backing materials to that of 5 mil-thick stainless-steel. The two transmittances were increased to 0.84 and 0.76 for 52 and 45 keV photons respectively.

Still higher transmittances were provided by samples electrodeposited on metallic foils and metallically-coated mylar. Sample backings of gold and nickel coated mylar, and foils of stainless-steel and copper were used to assess the merits of each. The Au-coated mylar had problems of flaking and uneven deposition, however, the Ni-coated mylar accepted the deposition quite evenly with very little noticeable tendency toward flaking. The stainless-steel and copper foils of 0.16 mil (3.19 mg/cm^2) and 0.15 mil (3.41 mg/cm^2) thickness respectively provided high-quality, evenly-deposited samples. Based upon visible quality and transmittance, the slight edge would go to the use of stainless-steel foil. The transmittance for 50 keV photons was 0.994 and that for 45 keV photons was 0.989. The copper foil provided for transmittances of 0.993 and 0.988 respectively for 52 and 45 keV photons.

Gamma-ray spectra were taken of the front sides of ^{239}Pu and ^{240}Pu samples in an attempt to identify the gamma ray that was to serve as the gating pulse for the alpha spectra. Repeated measurements failed to identify the gamma ray of interest. The USAF Radiological Health Lab ran one ^{239}Pu sample of approximately 500 DPM overnight on their planar Ge(Li) detector in a very low background chamber and were unable to identify the 52 keV gamma ray. Various attempts at gating off of the area of the spectrum corresponding to 52 keV yielded no significant coincident counts.

The reverse coincidence experiment of gating off the 5.15 MeV alpha group, when acquiring the gamma-ray spectrum of the sample, was performed in an attempt to reduce the background sufficiently to see the gamma-ray peak. These coincidence experiments permitted identification of the peak, but with only 3 counts under the peak, it could not be quantitatively analyzed.

Higher activity levels (1500 DPM) naturally produced more coincidences, but in a 48 hour acquisition period the number of coincident counts under a peak were still far too few to quantify the isotopic ratio.

Coincidence Spectroscopy Results

Based upon the total efficiencies for alpha particle and gamma-ray detectors used in this experiment, the gamma-ray intensities of ^{239}Pu and ^{240}Pu, and upon the background; the minimum activity levels for detection and quantification by this coincidence technique can be theoretically calculated. The average background count (μ_B) for coincidence spectroscopy over even extended counting periods of 48 hours was zero. Assuming the sample is deposited on one of the thin foils providing approximately 99% transmittance for 52 and 45 keV photons, the activity necessary (in DPM) for detection and quantification of a pure ^{239}Pu or ^{240}Pu source are tabulated in Table IV for various acquisition times.

Singles Spectroscopy Discussion

From equation (9), Chapter II, one observes that the accuracy of this method is very sensitive to the calculated x-ray to alpha emission ratio of the sample. Dividing both numerator and denominator of the

right hand side of this equation by α_T, the equation directly incorporates these ratios:

$$\frac{\alpha_{239}}{\alpha_{240}} = \frac{0.101 - \frac{X_T}{\alpha_T}}{\frac{X_T}{\alpha_T} - 0.046} \qquad (11)$$

This ratio of total L x-rays to alpha particles emitted will vary theoretically from 0.046 for pure ^{239}Pu to 0.101 for pure ^{240}Pu. A calculated ratio outside this range gives meaningless results. This experiment has been essentially concerned with measuring these ratios for the three major L-shell x-ray subgroups: L_α , L_β , L_γ . The samples measured, varied from 400 DPM to 1600 DPM. These samples, in some cases, possessed carrier isotopes and impurities of either ^{241}Am or ^{238}Pu, or both. Corrections to the L x-ray yields for their presence introduced still other errors and uncertainties in the final results.

Table IV

Minimum Sample Activities for Detection and Quantification in Coincidence Spectroscopy

	L_d (2.71 Counts)		L_q (100 Counts)	
Acquisition Time (Hrs)	^{239}Pu (DPM)	^{240}Pu (DPM)	^{239}Pu (DPM)	^{240}Pu (DPM)
1	10,893	4,728	401,977	174,480
4	2,723	1,182	100,494	43,620
8	1,362	592	50,247	21,810
16	681	295	25,123	10,905
24	453	197	16,749	7,270

The accuracy of the measured L x-ray to alpha ratios were dependent upon the total efficiencies and associated uncertainties for the

alpha particle and x-ray sample-detector combinations. Because of the fact that the area of deposition was larger than the Si(Li) detector entrance window, much of the sample was masked by the detector housing. This made the original assumption of an even distribution of activity over the deposition area very critical. The efficiencies in this case had relative standard deviations as high as 13%. It was felt that masking off the sample for alpha detection to the same central 7mm diameter area seen by the Si(Li) detector, would reduce the impact of uneven deposition on these calculated ratios. Rather than calculate efficiencies for both detectors with this new geometry, a total efficiency ratio ($\epsilon_{x\text{-ray}}/\epsilon_{\alpha}$) was calculated using a 0.1 μCi high purity ^{240}Pu source of the same geometry.

Singles Spectroscopy Results

Using the masked source for alpha spectroscopy, the calculated L x-ray to alpha emission ratios (absolute intensities) are tabulated in Table V for several samples of different isotopic content and activity. The uncertainties are the standard deviations and incorporate the statistical uncertainties in the total count.

For the purpose of demonstrating the relative sensitivity of L x-ray spectroscopy to gamma-ray spectroscopy, Table VI lists the minimum activities of ^{239}Pu or ^{240}Pu necessary for quantitative analysis (for a relative uncertainty of 10%) at several acquisition times. The background was dependent upon the activity of the sample and this was incorporated in the calculation using the detector efficiencies for this experiment.

Table V

Measured L X-Ray Intensities

Sample #		L x-ray/α (measured)	L x-ray/α (actual Ref:4)	% Error
Pu-01 (800 DPM ^{240}Pu)	L_α	0.0385±.0028	0.0378±.0006	+ 1.9
	L_β	0.0409±.0029	0.0484±.0007	-15.5
	L_γ	0.0104±.0019	0.0120±.0003	-13.3
	ΣL	0.0898±.0045	0.1006±.0010	-10.7
Pu-05 (1500 DPM ^{239}Pu)	L_α	0.0161±.0011	0.0182±.0004	-12.1
	L_β	0.0211±.0012	0.0216±.0004	- 2.3
	L_γ	0.0045±.0006	0.0053±.0001	-15.1
	ΣL	0.0417±.0017	0.0463±.0006	- 9.9
Pu-11 (400 DPM ^{240}Pu)	L_α	0.0438±.0036	0.0378±.0006	+15.8
	L_β	0.0501±.0038	0.0484±.0007	+ 3.3
	L_γ	0.0129±.0028	0.0120±.0003	+ 7.5
	ΣL	0.1068±.0059	0.1006±.0010	+ 6.2
Pu-13 (1300 DPM ^{240}Pu)	L_α	0.0382±.0026	0.0378±.0006	+ 0.5
	L_β	0.0521±.0031	0.0484±.0007	+ 7.4
	L_γ	0.0139±.0019	0.0120±.0003	+15.8
	ΣL	0.1042±.0045	0.1006±.0010	+ 3.6
Am-241 (650 DPM ^{241}Am)	L_α	0.1343±.0070	0.132 ±.003	+ 1.5
	L_β	0.1725±.0074	0.1925±.006	- 9.9
	L_γ	0.0316±.0038	0.0485±.002	-34.8
	ΣL	0.338 ±.014	0.382 ±.007	-11.5

Table VI

Minimum Sample Activities for Quantification

using L X-Ray Spectroscopy

Acquisition Time (Hrs)	^{239}Pu (DPM)	^{240}Pu (DPM)
1	29,409	13,414
4	7,352	3,354
8	3,676	1,677
12	2,451	1,118
16	1,838	838
24	1,225	559
48	612	279

Conclusions

Coincidence Spectroscopy. At the activity level of several hundred to several thousand disintegrations per minute of ^{239}Pu or ^{240}Pu, coincidence spectroscopy appears unfeasible. This is primarily due to the low abundance of gamma rays from the decay of these two isotopes. For alpha gated gamma-ray spectroscopy, the reduction in background possible in coincidence spectroscopy is more than offset by the inclusion of the efficiency of the alpha particle detector. This reduces the total number of coincident counts and increases the minimum activity for quantitative analysis. Based upon the background of the "singles" gamma-ray spectrum, the minimum activity of ^{239}Pu necessary to quantify the 52 keV gamma ray in one hour of acquisition is only 174,000 DPM (less than half that for coincidence spectroscopy). It is doubtful that increases in efficiency by larger geometries and higher intrinsic efficiencies could lower these minimum activities for coincidence spectroscopy by more than an order of

magnitude. These improvements, if possible, would still do little to improve the utility of the system for analysis of low-activity samples.

Singles Spectroscopy. The principle of determining ^{239}Pu to ^{240}Pu ratios by the different L x-ray to alpha yields is, in theory, possible. The calculations are very sensitive to errors in the calculated L x-ray to alpha ratio. It should be possible to reduce these errors to somewhere below 5% with better sample-detector geometry for x-ray detection. With a standard deviation error of 2% in the total L x-ray to alpha ratio (Ref 4:580) the standard deviation of the calculated $^{239}Pu/^{240}Pu$ ratio should be under 8% for a 50% activity contribution of each isotope. In conclusion, the sensitivity of the method is not as accurate as mass spectrometry (uncertainties are under 1% for sample activities as low as 100 DPM); however, it does provide an alternative method for computing the mass ratio of the two plutonium isotopes.

Recommendations

Results of the "singles" alpha and L x-ray spectroscopy approach have identified one primary improvement that is necessary in reducing the statistical and systematic errors in the measured L x-ray/alpha emission ratio. The improvement would be that of increasing the sample-detector geometry. A larger detector would increase the geometry factor and would, at the same time, reduce the sensitivity to irregularities in sample electrodeposition. The acquisition times would be lower and errors resulting from the counting statistics would be reduced.

Two semiconductor detector types are routinely used in x-ray spectroscopy: silicon, Si(Li), and germanium, Ge(Li) or intrinsic Ge. Each have their merits and demerits and each can be obtained in large surface areas (100-1000 mm^2).

Si(Li) detectors exhibit intrinsic efficiency curves that are essentially level at energies from 1 keV - 20 keV. Above 20 keV, the efficiency rapidly decreases with increasing energy. The energy at which the efficiency starts to decrease and its rate of decrease is dependent upon detector thickness. The silicon K x-ray escape probability is very small, at less than 1% for photons of 1-40 keV (Ref 16:2.12). A major disadvantage in the Si(Li) detector is that as the surface area of the detector increases, the resolution becomes much poorer than that of a comparable size germanium detector. The resolution for the 30 mm^2 detector used in this experiment was 205 eV FWHM at 6.4 keV. For a new Si(Li) detector of 500 mm^2, a resolution of only 500 eV FWHM at 6.4 keV can be expected.

Germanium detectors, both intrinsic and lithium-drifted, exhibit efficiency curves that fall off slowly on both ends of the energy spectrum. Below 20 keV, the efficiency falls with decreasing energy to a discontinuity at 11.1 keV; this is due to the K absorption edge of Ge. With increasing energy, the efficiency remains relatively level before falling off slowly at 60 keV. The rate of this decrease in efficiency is, as with the Si(Li) detector, dependent upon the thickness of the detector. The germanium K x-ray escape, however, cannot be neglected as in Si(Li) detectors, and is as high as 12% for a 15 keV incident photon (Ref 16:2.12). Germanium detectors have better resolution than Si(Li) as the detector area increases. Bemis et al. (Ref 4:580) report a resolution of 250 eV FWHM at 18 keV for a 1000 mm^2 intrinsic germanium detector. (see Fig. 10 for typical Si(Li) and Ge efficiency curves).

From the preceding discussion, it is obvious that a trade-off in resolution occurs as the surface area is increased. Nearly all

semiconductor-detector L x-ray spectra measured at an energy resolution of better than 1 keV FWHM can be broken down in four broad groups; the L_ℓ , L_α , L_β and L_γ groups, even though all L-series lines may not be readily identifiable. To identify the contribution of Np L x rays to a spectrum of U L x rays, however, requires a resolution better than 500 eV FWHM at approximately 18 keV.

Based upon these considerations, it would appear that cost would be the limiting factor on choice of detector size. The intrinsic germanium detector of 1000 mm^2 described by Bemis would provide for the best geometry, and its resolution would be comparable to the 30 mm^2 Si(Li) detectors. A high quality Si(Li) detector of 200 mm^2 surface area should however, provide sufficient resolution at a much lower cost, and yet increase the geometry greatly. Acquisition times or minimum activities for quantification could be reduced by one order of magnitude by an increase in detector area to 100 mm^2. Table VII reflects the minimum activity levels for quantification for a four-hour acquisition time that might be expected for Si(Li) detectors of various areas. For the purpose of table generation, the background was assumed to be similar to that of the detector used in this project yet was assumed to increase in proportion to surface area increases. The intrinsic photopeak efficiency was assumed to be unchanged from this experiment. Geometry factors for the detectors were calculated on the assumption that the entire sample could be seen by the detector and that the sample-detector distance was fixed at 5 mm.

Table VII

Minimum Sample Activities for Quantification using L X-Ray Spectroscopy for Various Detector Areas in a Four Hour Acquisition Period

Detector Area (mm^2)	^{239}Pu (DPM)	^{240}Pu (DPM)
80	622	285
100	612	280
200	495	225
300	380	174
500	295	135
800	253	115
1000	240	109

It is recommended that work be continued in analyzing the L x-ray spectra of mixed plutonium isotopes and in minimizing the errors in measured L x-ray intensities. A concentrated effort should be made toward establishing a rigid, reproducible source-detector geometry, with distance from source to detector determined to a high degree of accuracy. A chamber similar to that used in this project, but perhaps with a larger, thinner beryllium window, to accommodate the larger geometry, could provide such a sample mount. A cryogenically-cooled x-ray detector in a second vacuum chamber with similar beryllium window would allow simultaneous alpha and x-ray spectra acquisition (on an appropriate MCA) without the inconvenience of warming the detector and reevacuating the chamber when a sample was to be changed. Emphasis needs to be continued on this simultaneous acquisition if the procedure is to be reduced to that of a single measurement.

A computer program similar to that of SPECTRA should be developed to analyze the resulting complex x-ray spectra resulting from the presence of other heavy elements.

Research for this project has exposed the fact that little is presently known about the intensities of the L-series lines in each subgroup of Np characteristic x rays following the decay of ^{236}Pu. Further work on this project might well provide information on these intensities.

Bibliography

1. Lederer, C.M., et al. Table of Isotopes (Sixth Edition) New York: John Wiley and Sons Inc., 1967

2. Kaplan, I. "Gamma-Decay: Internal Conversion" in Nuclear Physics (Second Edition) Reading, Mass.: Addison-Wesley Publishing Co., 1964

3. Siegbahn, K. "The Coincidence Method" in Alpha-, Beta- and Gamma-Ray Spectroscopy. Vol. I. Amsterdam: North-Holland Publishing Co., 1966

4. Bemis, C. E., et al. "Detection of Internally Deposited Actinides, Part IV Preliminary Considerations in the Use of Large, Planar Intrinsic GE Detectors". Presented at the Ninth Midyear Topical Symposium of the Health Physics Society, Denver, Colo., Feb. 9-12, 1976

5. Toohey, R. E. "Relative Abundances of Uranium L α, β, γ Conversion X-Rays following the α-Decay of Plutonium". Preprint of summary of paper presented at the 21st annual meeting of the Health Physics Society, San Francisco, Calif. June 28-July 2, 1976.

6. Campbell, J. L. and L. A. McNelles. "An Inter-Comparison of Efficiency-Calibration Techniques for Semiconductor X-Ray Detectors". Nuclear Instruments and Methods, 125:205-223 (January 1975).

7. Watanabe, K., et al. "Radiochemical Determination of Plutonium Isotopes and Americium - 241 in a Plutonium Sample". Journal of Nuclear Science and Technology, 1, No. 6:197-202 (January 1964)

8. Bubernak, J., et al. "Determination of Americium in Plutonium by Gamma Counting". Analytical Chemistry, 30:1759 (1958)

9. Curtis, M. "Determination of PPM ^{236}Pu in ^{238}Pu by Alpha Pulse Height Analysis". Analytical Chemistry 40:1352 (July 1968)

10. Cline, J. E. "Level Structure of ^{235}U Observed by a Study of the Alpha Decay of ^{239}Pu". Nuclear Physics, A 106:481-496 (1968)

11. Hyde, E. K. et al. The Nuclear Properties of the Heavy Elements, Vol. II. Englewood-Cliffs, N.J.: Prentice-Hall, Inc., (1964)

12. Bevington, P. R. Data Reduction and Error Analysis for the Physical Sciences. New York: McGraw-Hill Book Co., (1969)

13. Snell, A. H. Nuclear Instruments and Their Uses New York: John Wiley and Sons Inc., (1962)

14. Currie, L. A. "Limits for Qualitative Detection and Quantitative Determination". Analytical Chemistry 40:586-593 (March 1968)

15. Heath, R. L. Scintillation Spectrometry-Gamma-Ray Spectrum Catalogue (Second Edition) IDO-16880-1 Washington, D.C.: U.S. GPO, (1964)

16. Woldseth, R. X-Ray Energy Spectrometry Burlingame, Calif: KEVEX Corporation, 1973

Appendix A:

Heavy Element Radiation Yields

Table VIII

Major Alpha and Photon Energies and Intensities

for Heavy Elements

Radiation	Energy	Absolute Yield
	^{236}Pu $t_{\frac{1}{2}}$=2.85 y	
α_0 (Ref 1)	5.769 MeV	0.69
α_{48}	5.722	0.31
α_{157}	5.616	0.0018
γ_1	47. keV	3.1×10^{-4} (a)
γ_2	110.	1.2×10^{-4}
γ_3	165.	6.6×10^{-6}
	^{238}Pu $t_{\frac{1}{2}}$= 86 y	
α_0	5.499 MeV	0.72
α_{43}	5.456	0.28
α_{143}	5.358	9.0×10^{-4}
L_ℓ (U) (Ref 4)	11.618 keV	0.0026
L_α (U)	13.615	0.0415
L_β (U)	17.220	0.0561
L_γ (U)	20.167	0.0136
γ_1	43.49	3.9×10^{-4} (a)
γ_2	99.87	7.4×10^{-5}
γ_3	152.77	1.01×10^{-5}

Table VIII (cont.)

^{242}Pu $t_{\frac{1}{2}}=3.79\times10^{5}$ y

Radiation	Energy	Absolute Yield
α_0 (Ref 1)	4.903 MeV	0.76
α_{45}	4.863	0.24
L_ℓ (U) (Ref 4)	11.618 keV	0.0021
L_α (U)	13.615	0.0310
L_β (U)	17.220	0.0415
L_γ (U)	20.167	0.0108
γ_1	44.92	3.3×10^{-4} (a)
γ_2	103.50	7.2×10^{-5}
γ_3	158.80	4.2×10^{-6}

^{243}Am $t_{\frac{1}{2}}=7.95\times10^{3}$ y

α_{75} (Ref 1)	5.276 MeV	0.879
α_{118}	5.234	0.106
α_{172}	5.181	0.011
α_0	5.350	0.0016
α_{31}	5.321	0.0012
γ_1	74.67 keV	0.660 (a)
γ_2	43.53	0.055
γ	86.7	0.0037
γ	117.8	0.0050
γ	142.0	0.0013

Table VIII (cont.)

Radiation	Energy	Absolute Yield
^{241}Am $t_{\frac{1}{2}}$=458 y		
α_{60} (Ref 1)	5.486 MeV	0.86
α_{103}	5.443	0.127
α_{159}	5.389	0.0139
α_{0}	5.545	0.0025
α_{33}	5.513	0.0012
L_{ℓ}(Np) (Ref 6)	11.898 keV	0.0086
L_{α}(Np)	13.944	0.132
L_{β}(Np)	17.750	0.1925
L_{γ}(Np)	20.785	0.0485
γ_{5}	59.54	0.359
γ_{7}	99.00	2.02×10^{-4}
γ_{8}	103.00	1.95×10^{-4}
γ_{9}	123.01	1.02×10^{-5}
γ_{10}	125.30	3.95×10^{-5}
^{246}Cm $t_{\frac{1}{2}}$=5.5x10^{3} y		
α_{0} (Ref 1)	5.386 MeV	0.81
α_{45}	5.342	0.19
L_{ℓ}(Pu) (Ref 4)	12.124 keV	0.0021
L_{α}(Pu)	14.279	0.0333
L_{β}(Pu)	18.294	0.0371
L_{γ}(Pu)	21.417	0.0086
γ	44.55	unknown (a)

Table VIII (cont.)

^{244}Cm $t_{\frac{1}{2}}$=17.6 y

Radiation	Energy	Absolute Yield
α_0 (Ref 1)	5.806 MeV	0.767
α_{43}	5.763	0.233
α_{142}	5.666	2.3×10^{-4}
L_ℓ(Pu) (Ref 4)	12.124	0.0025
L_α(Pu)	14.279	0.0386
L_β(Pu)	18.294	0.0430
L_γ(Pu)	21.417	0.0103
γ_1	42.82	2.0×10^{-4} (a)
γ_2	98.86	1.3×10^{-5}
γ_3	152.63	1.5×10^{-5}

(a) Argonne National Laboratory "Gamma-Rays by Nuclides" computer library listing

Appendix B:

Figures

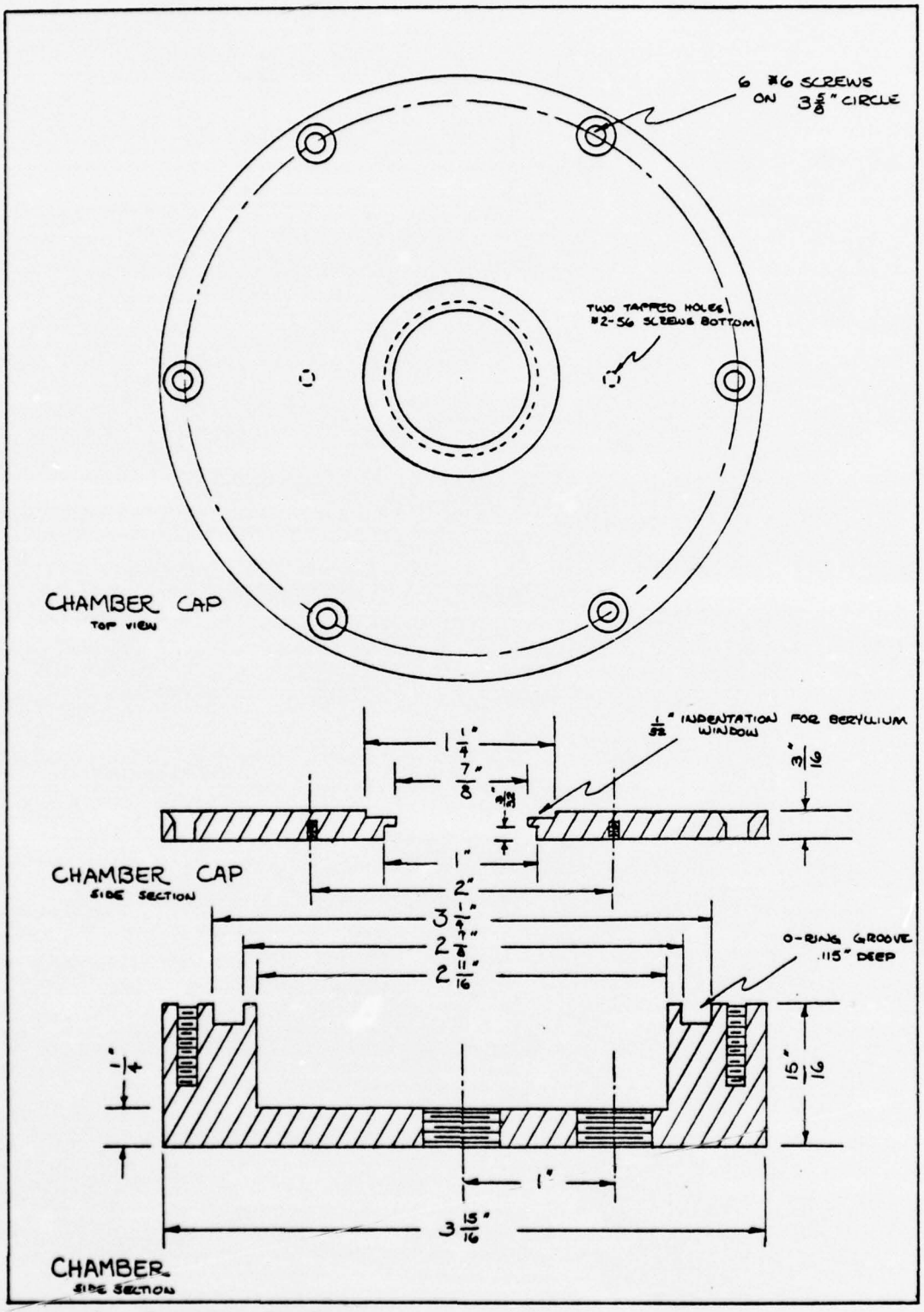

Figure 4. Detector Chamber

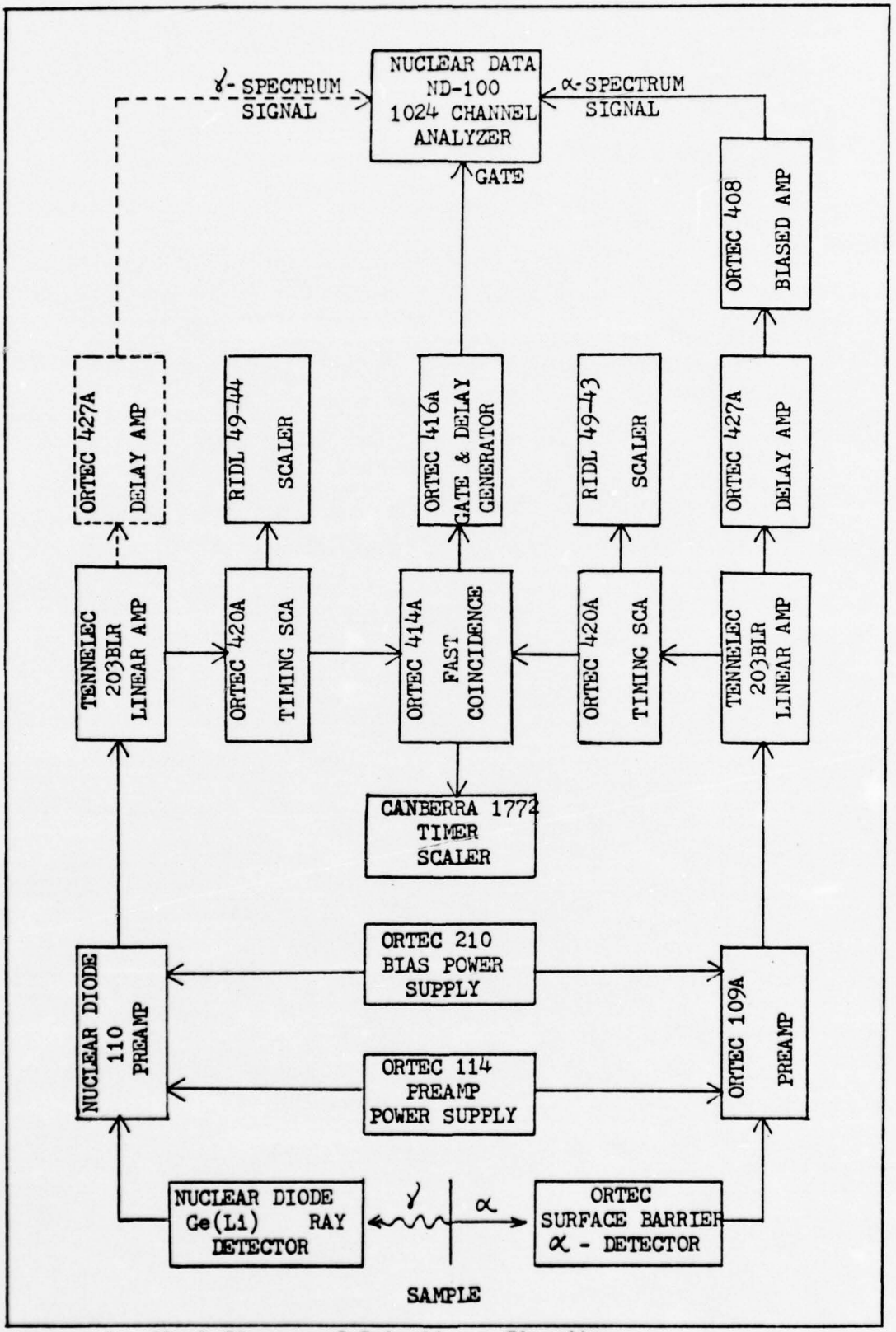

Figure 5. Block Diagram of Coincidence Circuitry

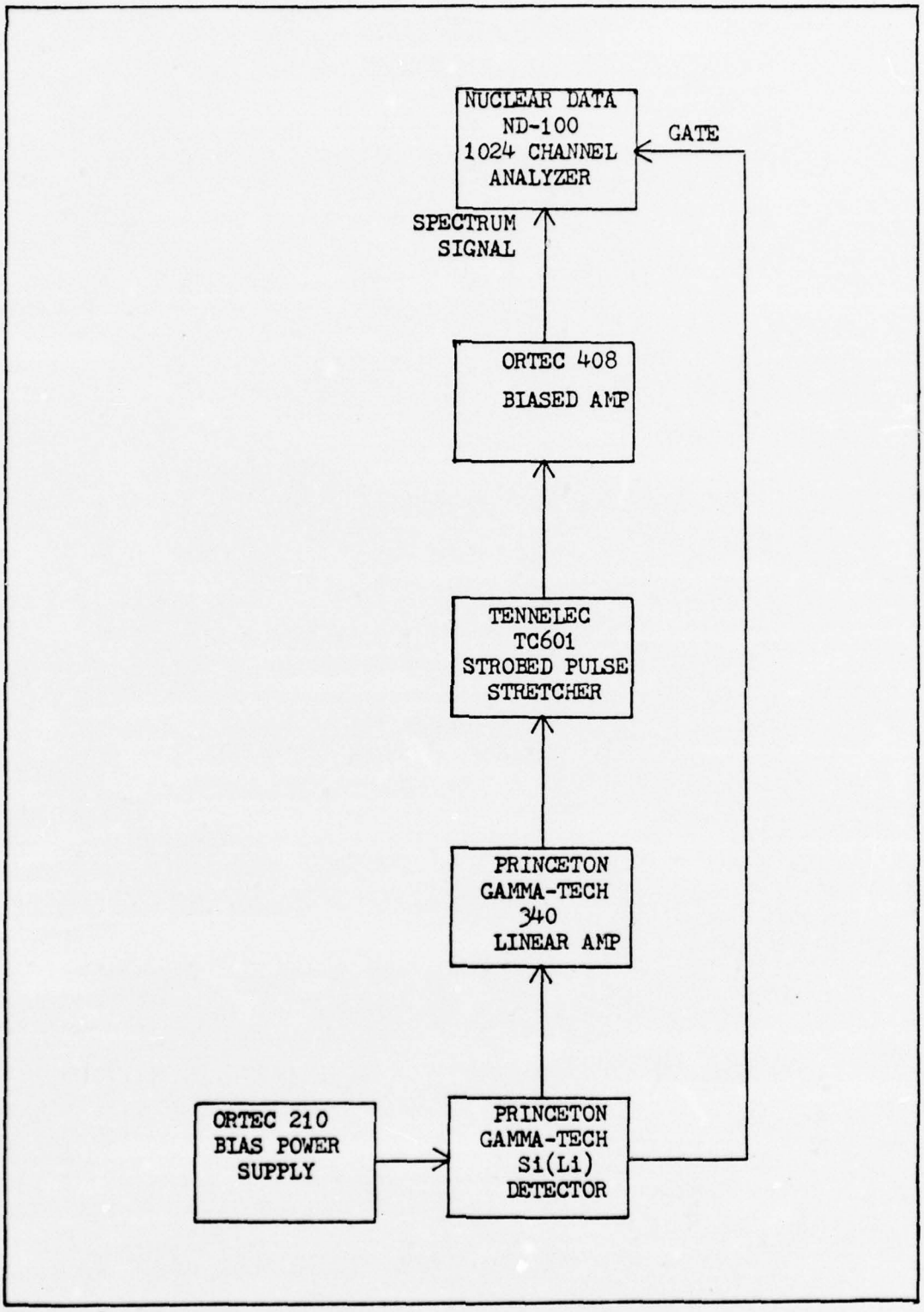

Figure 6. Block Diagram of X-Ray Spectroscopy Circuit

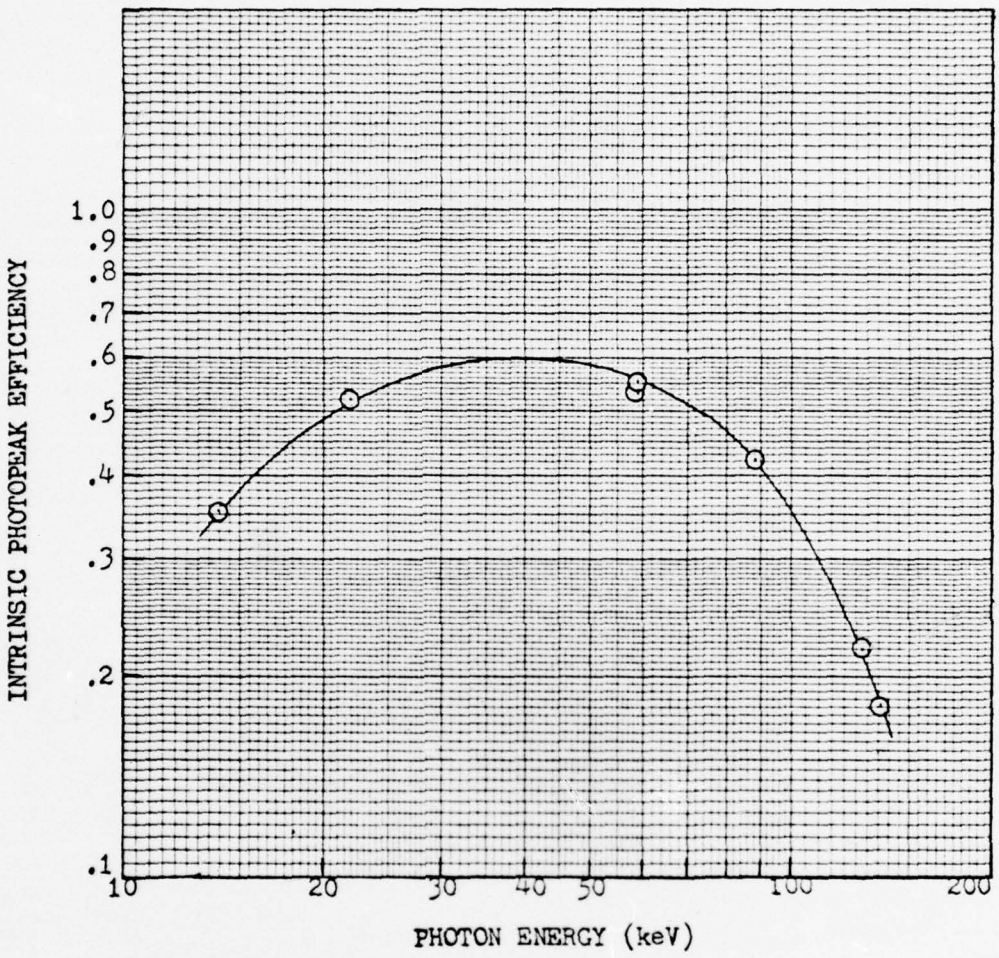

Figure 7. Intrinsic Photopeak Efficiency Curve for Nuclear Diode Ge(Li) Detector

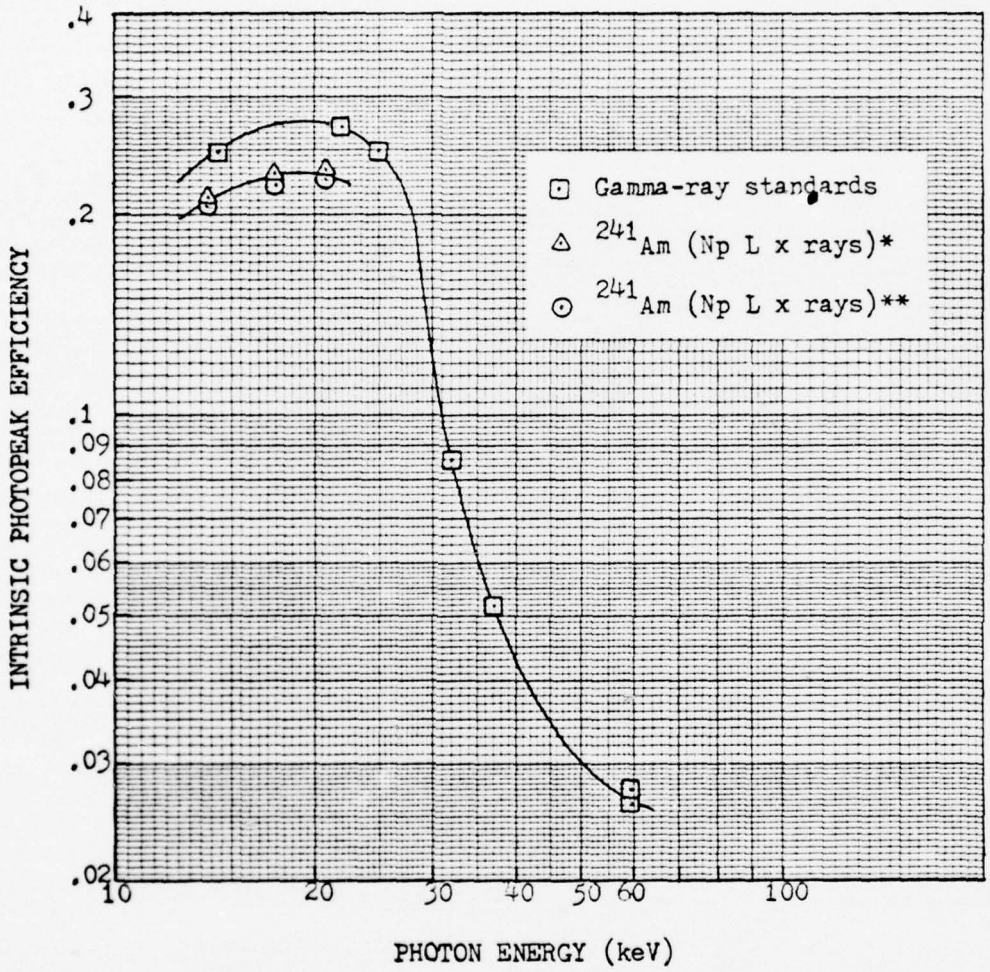

* MRC ^{241}Am standard

** NEN ^{241}Am standard

Figure 8. Intrinsic Photopeak Efficiency Curve for Princeton Gamma-Tech Si(Li) Detector

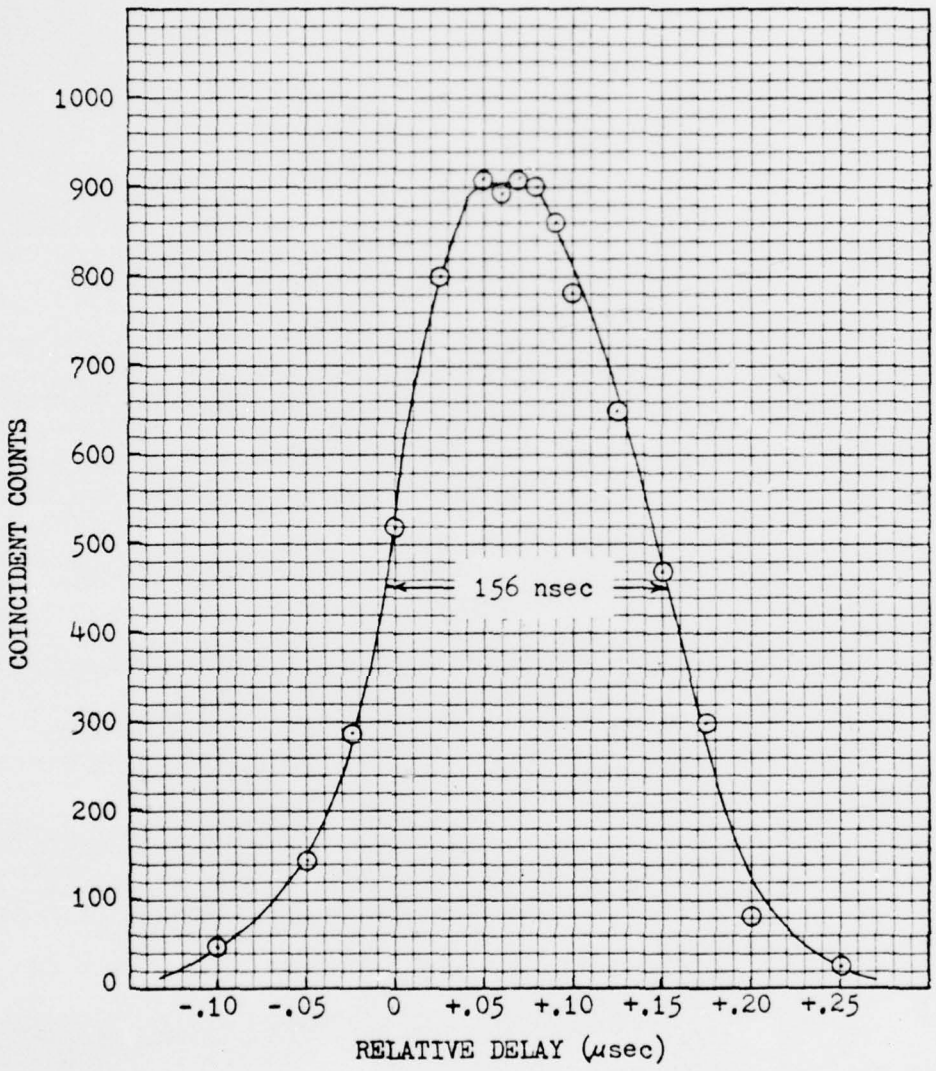

Figure 9. Coincidence Circuit Delay Curve

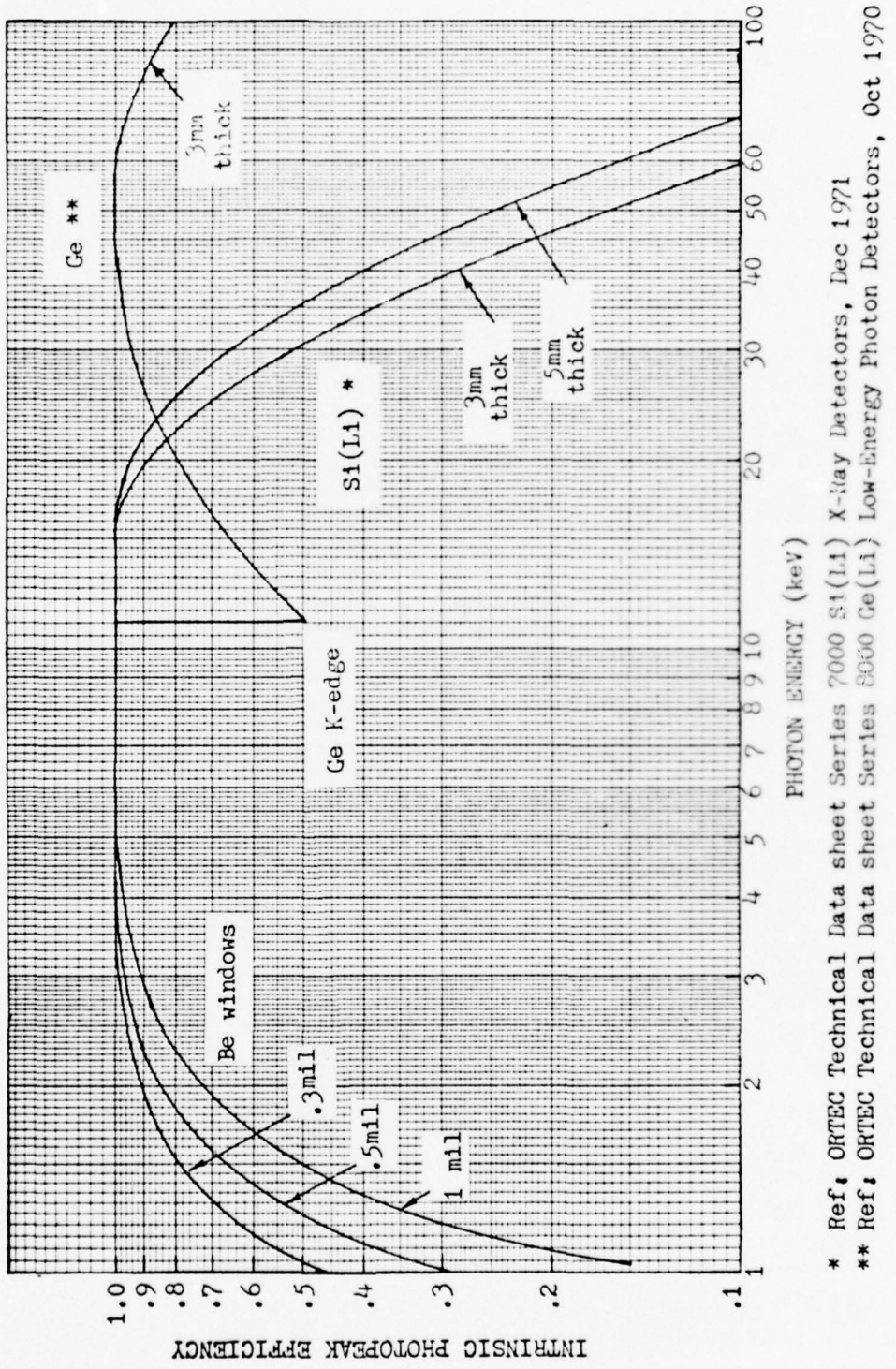

* Ref: ORTEC Technical Data sheet Series 7000 Si(Li) X-Ray Detectors, Dec 1971

** Ref: ORTEC Technical Data sheet Series 8000 Ge(Li) Low-Energy Photon Detectors, Oct 1970

Figure 10. Typical Si(Li) and Ge Efficiency Curves

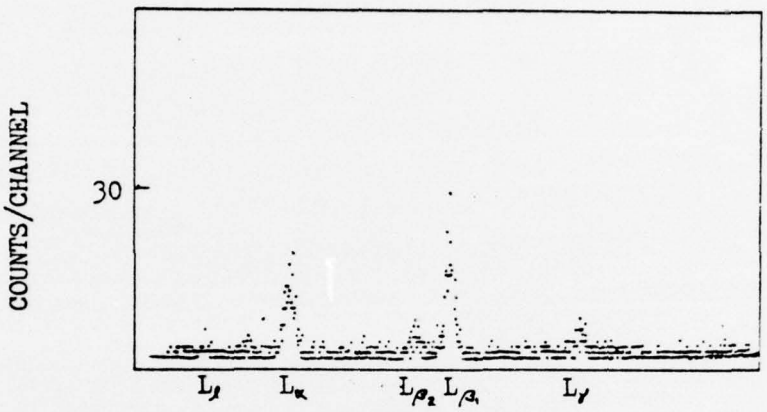

Figure 11. Typical Uranium L X-Ray Spectrum from Low-Activity ^{239}Pu Sample on Princeton Gamma-Tech Si(Li) Detector

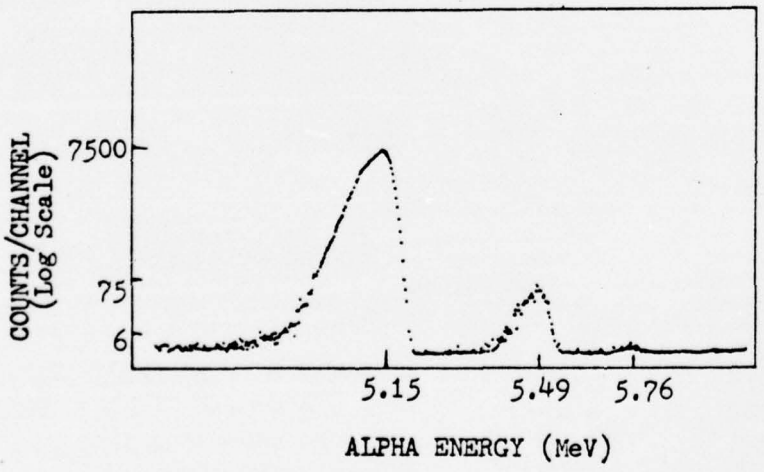

Figure 12. Typical ^{240}Pu Alpha Spectrum with ^{241}Am and ^{236}Pu Impurity Traces taken with 450 mm^2 ORTEC Ruggedized Silicon Surface-Barrier Detector

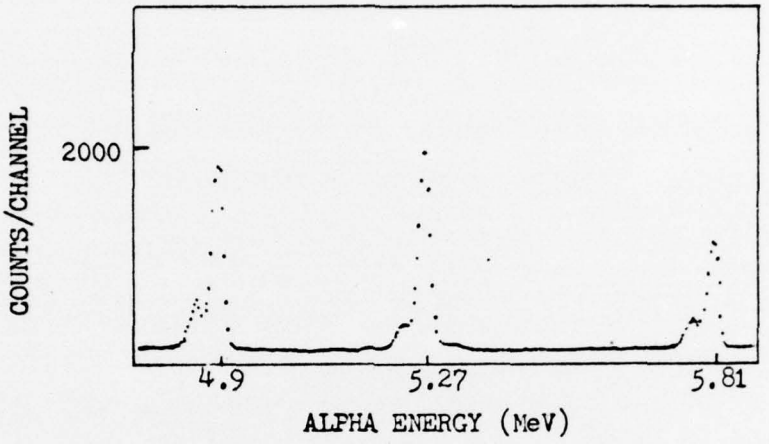

Figure 13. Typical Alpha Spectrum of Combined ^{242}Pu, ^{243}Am, and ^{244}Cm Sample on 100 mm^2 ORTEC Silicon Surface-Barrier Detector

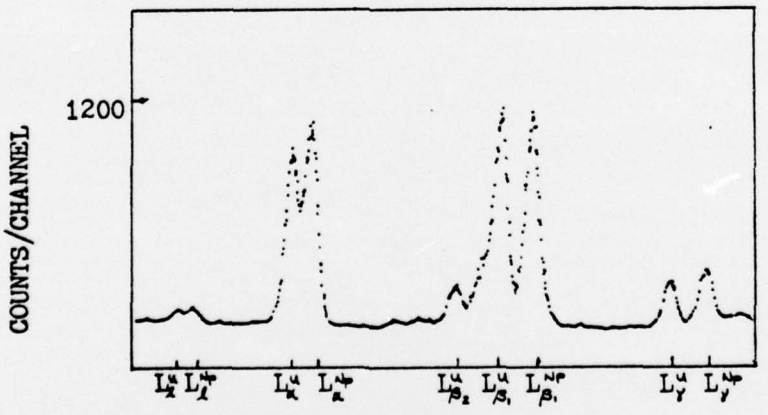

Figure 14. Typical Complex U/Np L X-Ray Spectrum from combined ^{239}Pu and ^{241}Am Sample taken with Princeton Gamma-Tech Si(Li) Detector

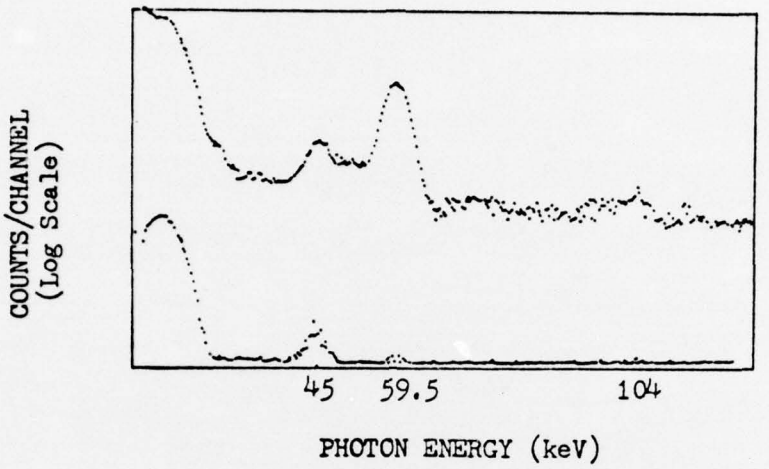

Top: Ungated Singles Gamma-Ray Spectrum of combined ^{240}Pu and ^{241}Am Sample

Bottom: 5.15 MeV alpha Gated Gamma-Ray Coincidence spectrum of combined ^{240}Pu and ^{241}Am Sample

Figure 15. Singles Gamma vs. Coincidence Gamma-Ray Spectrum for combined ^{240}Pu and ^{241}Am Sample taken with ORTEC 450 mm^2 Silicon Surface-Barrier Detector for Alpha Particles and Nuclear Diode Ge(Li) Detector for Gamma Rays.

APPENDIX C

GEOMETRY FACTOR FOR AN EXTENDED DISK SOURCE ON AXIS WITH A DISK DETECTOR

Many of the source-detector geometries with which this project dealt, could not be accurately approximated by point source geometries. A simple program that would calculate this geometry factor given the radii of detector and source and the distance between them, proved to be of value in determining detector efficiencies.

The approach taken was to simplify the expression presented by Heath (Ref 15:21) for the energy-dependent efficiency of a disk source on axis with a cylindrical detector:

$$T(E) = \frac{1}{\pi R_s^2} \int_0^{R_s} x\,dx \int_{-\frac{\pi}{2}}^{\frac{\pi}{2}} d\phi \left\{ \int_0^{\tan^{-1}\left(\frac{-x\sin\phi + \sqrt{x^2\sin^2\phi - (x^2 - R_d^2)}}{h+t}\right)} \left[1 - e^{-\mu(E)\frac{t}{\cos\theta}}\right] \sin\theta\,d\theta \right.$$

(12)

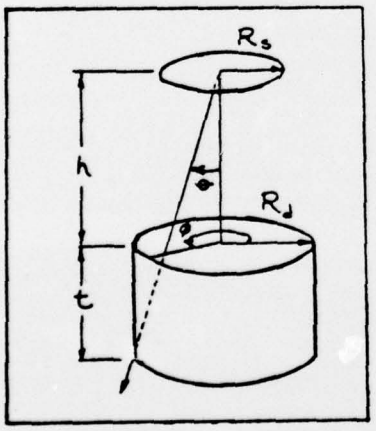

$$\left. + \int_{\tan^{-1}\left(\frac{-x\sin\phi + \sqrt{x^2\sin^2\phi - (x^2 - R_d^2)}}{h+t}\right)}^{\tan^{-1}\left(\frac{-x\sin\phi + \sqrt{x^2\sin^2\phi - (x^2 - R_d^2)}}{h}\right)} \left[1 - e^{-\mu(E)\left(\frac{-x\sin\phi + \sqrt{x^2\sin^2\phi - (x^2 - R_d^2)}}{\sin\theta} - \frac{h}{\cos\theta}\right)}\right] \sin\theta\,d\theta \right\}$$

The energy dependence of the equation can be removed by setting the square bracketed terms under the integrals equal to one. These are the probabilities (as a function of distance) that the radiation will be absorbed. Then, by taking the limit at $t \rightarrow 0$ (for an infinitely thin

detector), equation (12) simplifies to the geometry factor (GF) efficiency

$$GF = \frac{1}{\pi R_s^2} \int_0^{R_s} x\,dx \int_{-\frac{\pi}{2}}^{\frac{\pi}{2}} d\phi \int_0^{\tan^{-1}\left(\frac{-x\sin\phi + \sqrt{x^2\sin^2\phi - (x^2 - R_d^2)}}{h}\right)} \sin\theta\,d\theta \qquad (13)$$

Integrating over 0 the triple integral is reduced to the double integral:

$$GF = \frac{1}{\pi R_s^2} \int_0^{R_s} x\,dx \int_{-\frac{\pi}{2}}^{\frac{\pi}{2}} \left\{1 - \cos\left[\tan^{-1}\left(\frac{-x\sin\phi + \sqrt{x^2\sin^2\phi - (x^2 - R_d^2)}}{h}\right)\right]\right\} d\phi \qquad (14)$$

simplifying this integral provides:

$$GF = \frac{1}{2} - \frac{1}{\pi R_s^2} \int_0^{R_s} x\,dx \int_{-\frac{\pi}{2}}^{\frac{\pi}{2}} \cos\left[\tan^{-1}\left(\frac{-x\sin\phi + \sqrt{x^2\sin^2\phi - (x^2 - R_d^2)}}{h}\right)\right] d\phi \qquad (15)$$

This double integral was then solved by calling on AFIT Subroutine SIMPD which solves double integrals by Simpson's Rule iteration. The ource program follows in this Appendix.

```
      PROGRAM SOLIDA(INPUT=/80,OUTPUT)
      COMMON /1/ RD,H
C THIS PROGRAM COMPUTES THE GEOMETRY FACTOR FOR A
C CIRCULAR DISK SOURCE A GIVEN DISTANCE AWAY AND
C ON AXIS WITH A CIRCULAR DISK DETECTOR.
C WHERE: RS=SOURCE RADIUS
C        RD=DETECTOR RADIUS
C        H=DISTANCE FROM SOURCE TO DETECTOR
      PI=3.14159265358979323846
    5 READ*,RS,RD,H
      IF (EOF(5LINPUT)) 99,10,99
   10 PRINT*,"SOURCE RADIUS IN MM=",RS
      PRINT*,"DETECTOR RADIUS IN MM=",RD
      PRINT*,"DISTANCE FROM SOURCE TO DETECTOR IN MM=",H
      A1=-PI/2.
      B1=PI/2.
      A2=0
      B2=RS
      CALL SIMPD(A1,B1,A2,B2,.001,.001,100,100,2,2,ANSQ,
     1ALARM,JTOL)
      PRINT*,"ALARM=",ALARM,  "JTOL=",JTOL
      SOA=1./2.-ANSQ/(PI*RS**2)
      PRINT*,"THE GEOMETRY FACTOR IS:",SOA
   20 PRINT*,"**************************************"
      GO TO 5
   99 STOP
      END



      SUBROUTINE FNEVAL (PHI,FPHIX)
      COMMON X
      COMMON /1/ RD,H
      FPHIX=X*COS(ATAN((-X*SIN(PHI)
     &+SQRT(ABS(X**2*(SIN(PHI))**2-(X**2-RD**2))))/H))
      RETURN
      END
```

APPENDIX D

SPECTRA - A PROGRAM TO PRODUCE A THEORETICAL L X-RAY SPECTRUM FROM THE SUM OF GAUSSIAN PEAKS AND LEAST-SQUARES FIT BACKGROUND

Program SPECTRA was written to provide a method of correcting a complex L x-ray spectrum for the presence of other nuclides. Given a magnitude and energy of a reference peak, the program takes the energies and relative intensities of a series of L-shell lines; fits Gaussian peaks to these x rays and sums them to provide a theoretical spectrum. Given the background count at respective channel numbers, SPECTRA calls on a third degree polynomial least-squares fit to the background points (AFIT Subroutine PLSQ); adds the background to the theoretical spectrum, then subtracts that total spectrum from an experimental spectrum read into the program on data cards. The resulting spectrum, then, consists of the peaks of interest. Given areas of interest, SPECTRA then sums the counts under the resulting peaks.

FUNCTION PGAUSS (Ref 12:45) provides the Gaussian curve as a function of energy and standard deviation. The standard deviation also depends upon the energy of the peak and is provided to PGAUSS through FUNCTION SIG. The standard deviation is proportional to the square root of the energy. The constant of proportionality in SIG is supplied by the user and is dependent upon total detector system resolution.

Fig. 16 depicts a theoretical Np L x-ray spectrum and background arising from the decay of ^{241}Am. The relative intensities and energies of the 16 L-shell lines used to construct this spectrum were taken from Hyde et al. (Ref 11:853). Fig. 17 shows this same spectrum fit to the Np L x-ray peaks in a complex U/Np L x-ray spectrum. Fig. 18 provides the net U L x-ray spectrum after subtracting the background and Np spectrum.

```
      PROGRAM SPECTRA(INPUT=/80,OUTPUT,PLOT)
C THIS PROGRAM COMPUTES AND PLOTS A GAUSSIAN DISTRIBUTION
C FOR AN ENERGY PEAK GIVEN THE MEAN ENERGY, AND RELATIVE
C INTENSITY OF EACH PEAK IN THE SUBGROUP AND THE MAGNITUDE
C OF THE HIGHEST PEAK IN THE SUBGROUP.  THE PROGRAM THEN
C SUMS THE INDIVIDUAL GAUSSIANS AND PLOTS THE TOTAL SPECTRUM
      DIMENSION GA(1030),XC(1030),SPEC(1030),BKGS(1030)
      DIMENSION XB(9),YB(9),CB(4)
      DIMENSION SPECIN(1030),SSPEC(1030)
    1 FORMAT(1H ,10(1PE13.4)/10(1PE13.4))
    2 FORMAT(1H ,F6.2,5X,1PE13.4)
    8 FORMAT (1F6.0,9F8.0)
    9 FORMAT (1H ,10F13.0 /10(F13.0))
      SLOPE=.0136479758
      YINCPT=10.2468013
      GA(1025)=1.    $  SPEC(1025)=1.    $ BKGS(1025)=1.
      GA(1026)=1.       $ SPEC(1026)=1.    $ BKGS(1026)=1.
      READ 8,(SPECIN(I),I=1,1024)
      DO 91 I=1,1023
   91 SPECIN(I)=SPECIN(I+1)
      READ*,N
      DO 3 I=1,N
    3 READ*,XB(I),YB(I)
      CALL PLSQ(XB,YB,N,3,CB,0,EMAX,ERMS,EMEQ)
      DO 4 I=1,1024
      X=FLOAT(I)
      XC(I)=FLOAT(I)
    4 BKGS(I)=CB(1)*X**3+CB(2)*X**2+CB(3)*X+CB(4)
    5 READ*,NPKS,PKMAG
      IF(EOF(5LINPUT))199,7,199
    7 DO 80 L=1,NPKS
      READ*,EAVG,RI
      PRINT*,"********** PEAK NUMBER ",K+1," DATA *********"
      PRINT*,"      PEAK ENERGY=",EAVG," KEV"
      PRINT*,"      PEAK RELATIVE INTENSITY=",RI
      PRINT*,"      PEAK MAGNITUDE=",PKMAG*RI," COUNTS"
      SIG=SIGMA(EAVG)
      PRINT*,"SIGMA=",SIG
      PRINT*,"FWHM=",2.35*SIG,"KEV"
      SUM=0
      DO 10 I=1,100
      X=EAVG-3.*SIG+.06*I*SIG
      RJ=(X-YINCPT)/SLOPE
      J=RJ
      IF((RJ-J).GE..5) J=RJ+1
   10 GA(J)=PKMAG*RI*SIG*PGAUSS(X,EAVG,SIG)/.3989422804
      DO 20 I=1,1023
   20 SUM=SUM+(GA(I)+GA(I+1))/2.
```

```
      PRINT*,'TOTAL COUNTS UNDER GAUSSIAN=',SUM
      IF (K.GE.1) GO TO 60
      CALL PLOT(4.,1.,-3)
      CALL SCALE(XC,6.0,1024,1)
      CALL AXIS(0.,0.,14HCHANNEL NUMBER,-14,6.0,0,XC(1025)
     &,XC(1026))
      CALL LGAXIS(0.,0.,16HCOUNTS / CHANNEL,16,5.,90.,
     &GA(1025),GA(1026))
   60 DO 25 I=1,1024
      SPEC(I)=GA(I)+SPEC(I)
      IF(BKGS(I).LE.1.) BKGS(I)=1.
   25 IF(GA(I).LE.1.) GA(I)=1.
      CALL LGLINE(XC,GA,1024,0,1,1)
      DO 30 J=1,1024
   30 GA(J)=0
      K=K+1
   80 CONTINUE
   99 PRINT*,'THE TOTAL SPECTRUM'
      DO 40 J=1,1024
      SPEC(J)=SPEC(J)+BKGS(J)
   40 SSPEC(J)=SPECIN(J)-SPEC(J)
      PRINT 1,(SPEC(J),J=1,1024)
      READ*,NSEC
      DO 100 L=1,NSEC
      SECS=0
      RSECS=0
      READ*,N1,N2
      DO 101 K=N1,N2
      RSECS=RSECS+SSPEC(K)
  101 SECS=SECS+SPEC(K)
      PRINT*,'SUM COUNTS CH.',N1,' TO CH.',N2,'= ',SECS
      PRINT*,'THE REMAINING SUM COUNTS AFTER STRIPPING '
  100 PRINT*,'CHANNEL',N1,' TO CHANNEL',N2,'= ',RSECS
      CALL LGLINE(XC,BKGS,1024,-100,4,1)
      CALL LGLINE(XC,SPEC,1024,-0,3,1)
      CALL PLOT(9.,0.,-3)
   87 DO 88 I=1,1024
      IF (SSPEC(I).LE.1.) SSPEC(I)=1.
   88 IF(SPECIN(I).LE.1.) SPECIN(I)=1.
      PRINT 9,(SPECIN(I),I=100,200)
      SPECIN(1025)=1.
      SSPEC(1025)=1.
      SPECIN(1026)=1.
      SSPEC(1026)=1.
      CALL AXIS(0.,0.,14HCHANNEL NUMBER,-14,6.0,0,XC(1025),
     &XC(1026))
      CALL LGAXIS(0.,0.,16HCOUNTS / CHANNEL,16,5.,90.,
     &GA(1025),GA(1026))
```

```
      CALL LGLINE(XC,SPEC,1024,-0,3,1)
      CALL LGLINE(XC,SPECIN,1024,-2,3,1)
      CALL PLOT(9.,0.,-3)
      CALL AXIS(0.,0.,14HCHANNEL NUMBER,-14,6.0,0,XC(1025),
     &XC(1026))
      CALL LGAXIS(0.,0.,16HCOUNTS / CHANNEL,16,5.,90.,
     &GA(1025),GA(1026))
      CALL LGLINE(XC,SSPEC,1024,-0,3,1)
      CALL PLOT(9.,0.,-3)
      CALL PLOTE
  199 STOP
      END



      FUNCTION PGAUSS(X,EAVG,SIG)
      DOUBLE PRECISION Z
      Z=(X-EAVG)/SIG
      PGAUSS=.3989422804/SIG*DEXP(-(Z**2)/2.)
      RETURN
      END



      FUNCTION SIGMA(EAVG)
      F=EXP(.06071*EAVG-3.08116)
      SIGMA=3.6*SQRT(.0029*EAVG*F)/2.35
      RETURN
      END
```

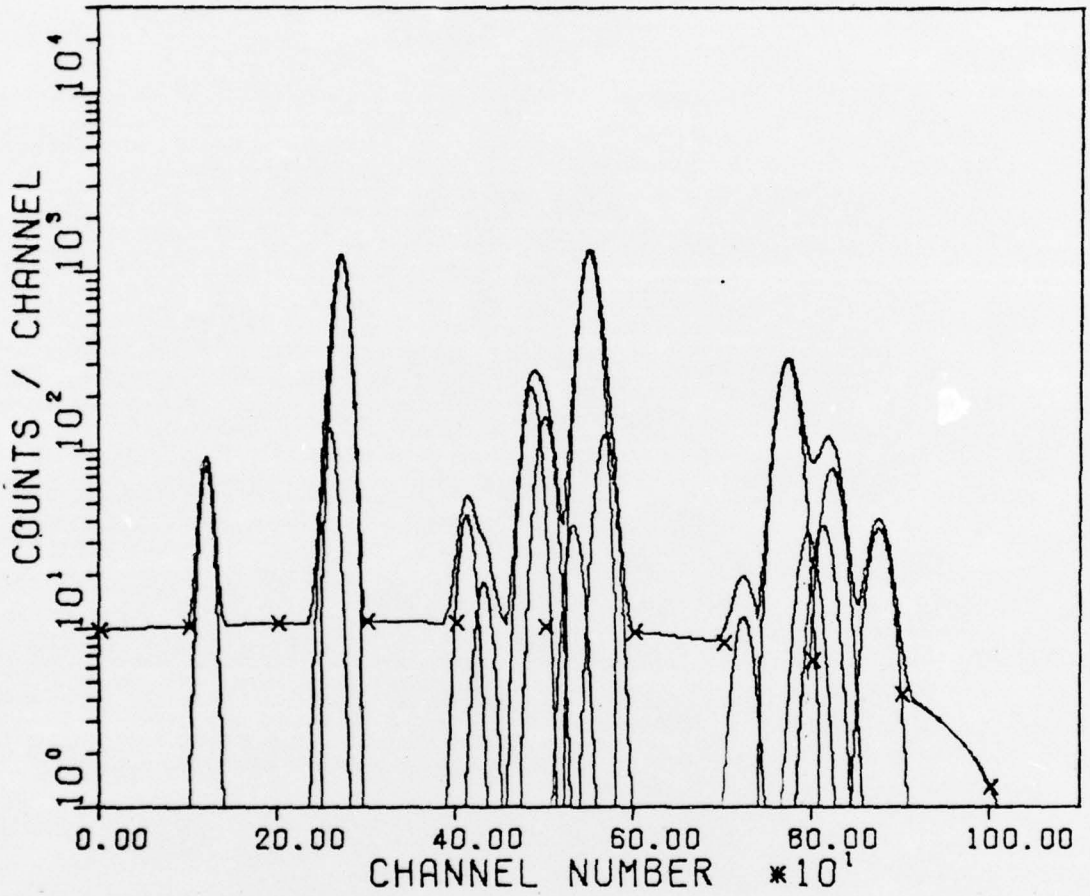

Figure 16. Theoretical Caussian-Fit Spectrum for Np L X Rays Following Decay of ^{241}Am

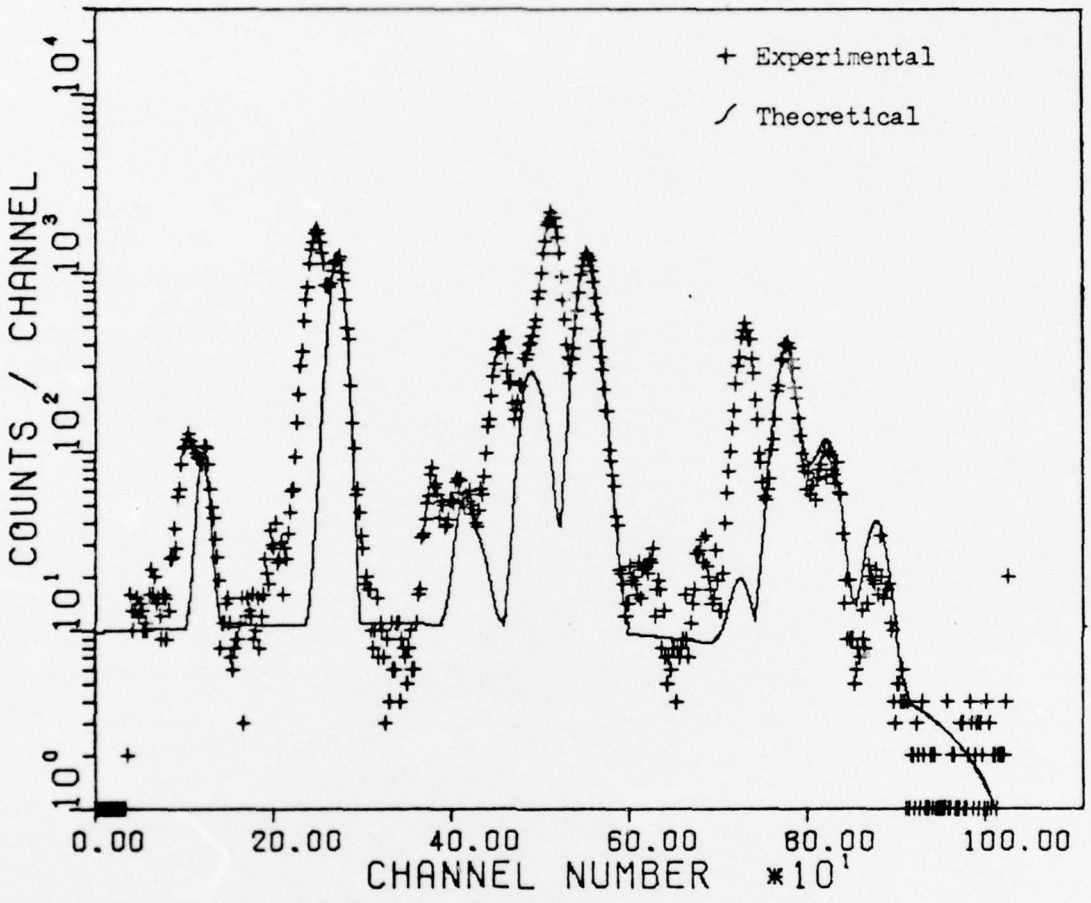

Figure 17. Theoretical Fit of Np L X-Ray Spectrum to Experimental Complex Np/U Spectra

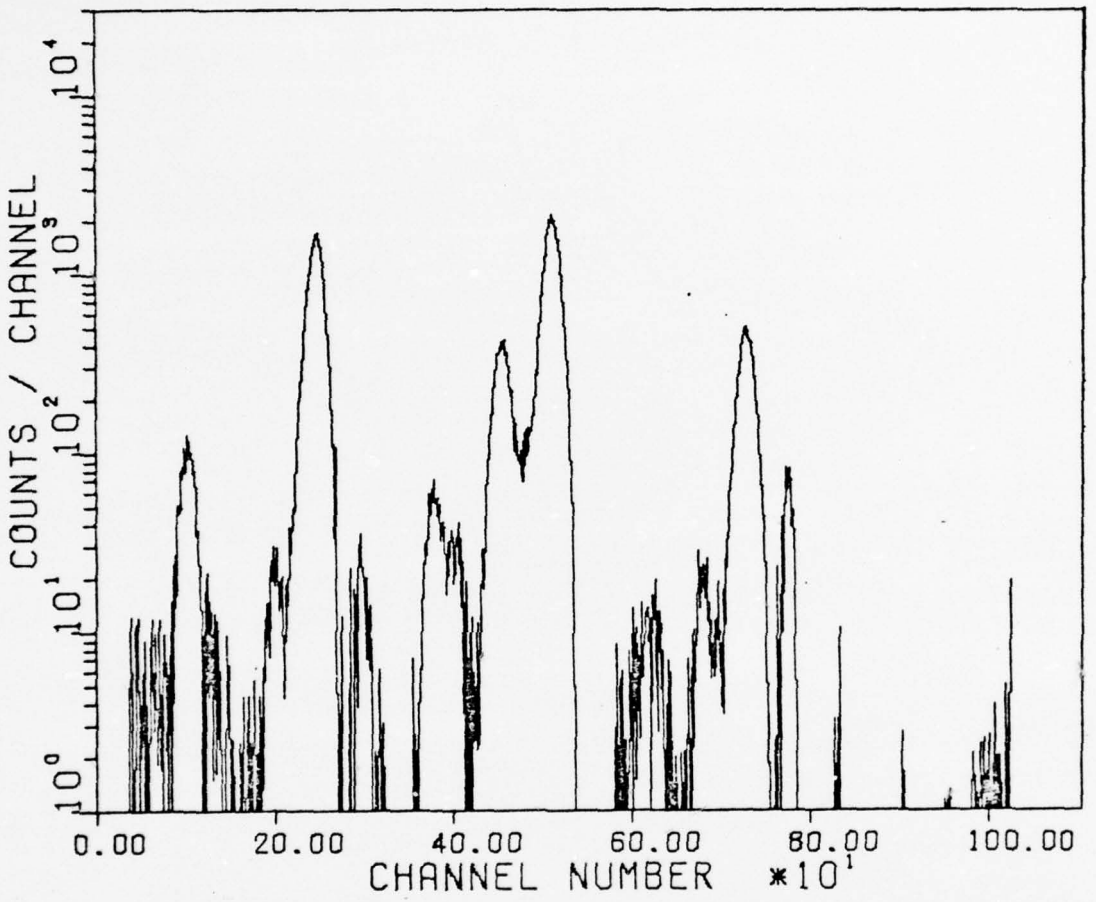

Figure 18. Uranium L X-Ray Spectrum after Stripping away Neptunium L X-Ray Spectrum from Complex Spectra

VITA

Jack Lee Strickland was born on 8 October 1945 in Panama City, Florida. After graduating from Bay County High School in 1963, he entered Gulf Coast Community College in Panama City. One year later, he entered the United States Air Force Academy in Colorado. He graduated with a Bachelor of Science degree in Engineering Sciences and was commissioned a 2nd Lieutenant in June 1968.

Capt. Strickland entered active duty in the Air Force at Williams AFB, Arizona and graduated from Undergraduate Pilot Training in 1969. Prior to entry into the Air Force Institute of Technology in June 1975, he was assigned to the Pacific Air Forces and Strategic Air Command with duty stations at Bien Hoa AB, South Vietnam; Andersen AFB, Guam; and Robins AFB, Georgia.

Permanent address: 111 N. Lakewood Dr.
Panama City, Florida 32401

UNCLASSIFIED

SECURITY CLASSIFICATION OF THIS PAGE (When Data Entered)

AFIT REPORT DOCUMENTATION PAGE		READ INSTRUCTIONS BEFORE COMPLETING FORM
REPORT NUMBER: GNE/PH/76D-7	2. GOVT ACCESSION NO.	3. RECIPIENT'S CATALOG NUMBER
4. TITLE (and Subtitle): ISOTOPIC ANALYSIS OF LOW-ACTIVITY PLUTONIUM SAMPLES USING HIGH-RESOLUTION ALPHA AND PHOTON SPECTROSCOPY.		5. TYPE OF REPORT & PERIOD COVERED: MS Thesis
		6. PERFORMING ORG. REPORT NUMBER:
7. AUTHOR(s): Jack L. Strickland, Captain		8. CONTRACT OR GRANT NUMBER(s): Master's thesis
9. PERFORMING ORGANIZATION NAME AND ADDRESS: Air Force Institute of Technology (AFIT-EN) Wright-Patterson AFB, Ohio 45433		10. PROGRAM ELEMENT, PROJECT, TASK AREA & WORK UNIT NUMBERS
11. CONTROLLING OFFICE NAME AND ADDRESS: McClellan Central Laboratory (MCLN) 1155th Technical Operations Squadron McClellan AFB, CA 95652		12. REPORT DATE: December, 1976
		13. NUMBER OF PAGES: 84
14. MONITORING AGENCY NAME & ADDRESS (if different from Controlling Office): 85p.		15. SECURITY CLASS. (of this report): Unclassified
		15a. DECLASSIFICATION/DOWNGRADING SCHEDULE

16. DISTRIBUTION STATEMENT (of this Report)

Approved for public release; distribution unlimited

17. DISTRIBUTION STATEMENT (of the abstract entered in Block 20, if different from Report)

Approved for public release; IAW AFR 190-17

JERRAL F. GUESS, Captain USAF
Director of Information

18. SUPPLEMENTARY NOTES

19. KEY WORDS (Continue on reverse side if necessary and identify by block number)

Isotopic Analysis
Plutonium 239, Plutonium 240
Alpha Spectroscopy
L-Shell X-Rays

20. ABSTRACT (Continue on reverse side if necessary and identify by block number)

High-resolution alpha particle and photon spectroscopy is applied to determining the ratios of ^{239}Pu and ^{240}Pu in isotopically mixed samples of less than a few thousand DPM. The utility of alpha-gamma coincidence and L-shell x-ray spectroscopy methods are explored. Experimental equipment, procedures and calibration methods are discussed. Minimum sample activities necessary for quantification are presented for each method. Instrumental and statistical uncertainties prevented reliable determination of isotopic ratios. Improvements in equipment are recommended to reduce uncertainties.

DD FORM 1 JAN 73 1473 EDITION OF 1 NOV 65 IS OBSOLETE

UNCLASSIFIED

SECURITY CLASSIFICATION OF THIS PAGE (When Data Entered)

012.225